

Study of 8" PMTs at UCLA For Pierre-Auger Surface Detectors

**Arun Tripathi, Chris DiPasquale, David Barnhill, Chris Jillings,
Shimul Akhanjee, Marisol Diaz, Louis Levenson, Jun Uehara,
William Slater, Katsushi Arisaka**

*University of California, Los Angeles
Department of Physics and Astronomy
Los Angeles, California 90095*

October 12, 2000

Abstract

We have tested three candidate PMT's for the Surface Array Detectors for the Pierre-Auger Observatory, being constructed in Malargue, Argentina. These are 8-inch PMT's from Hamamatsu (R5912) and ETL (9353KB), and 9-inch PMT's from Photonis (XP1802/FLB). We have developed dedicated systems to measure Quantum Efficiency (QE) and Linearity. In addition, basic quantities such as Gain, Dark current, Single Photo-electron spectrum, Dark Pulse Rate, and Afterpulse ratio etc. have been measured. We found that most of specifications required by the Auger Project can be met with existing PMT's. However, better linearity at low gain operation (at $\sim 10^5$) may require modifications such as reduction in the number of dynode stages.

Table of Contents

1. Introduction	3
1.1 THE PIERRE-AUGER COSMIC RAY OBSERVATORY	3
1.2 REQUIREMENT FOR SURFACE DETECTOR PMT'S	4
2. Measurements	4
2.1 QUANTUM EFFICIENCY	5
2.1.1 System Setup	5
2.1.2 Data Taking and Results	7
2.1.3 Discussion	10
2.2 GAIN AND DARK CURRENT	12
2.2.1 Absolute Gain Measurement by Single PE Peak	12
2.2.2 Dark Current and DC Gain measurement	15
2.2.4 Data Taking and Result	17
2.3 LINEARITY	18
2.3.1 System Setup	19
2.3.2 Data Taking and Results	20
2.4 DARK PULSE RATE	25
2.5 AFTERPULSE RATIO	27
3 Summary	29
4 Conclusion	30
5 Acknowledgements	31
6 References	31
Appendix A	32
A.1 Linearity System Setup	32
A.2 System Overview	32
A.3 System Specifics	33
Appendix B	39
B.1 Base Design for EMI PMT's (Negative HV)	39
B.2 Base Design for EMI PMT's (Positive HV)	40
B.3 Base Design for Hamamatsu PMT's (Negative HV)	41
B.5 Base Design for Photonis PMT's (Negative HV)	42

1. Introduction

1.1 The Pierre-Auger Cosmic Ray Observatory

The Pierre-Auger cosmic ray observatory is a detector designed to detect ultra high-energy cosmic rays. The primary objective of the Auger detector is to collect a high statistics sample of ultra high-energy (10^{20} eV) cosmic ray events, whose origin and the mechanism of acceleration still remains a mystery.

Two techniques have been used so far to detect and measure the energy of cosmic rays. One technique is to detect the fluorescent light produced by the N_2 molecules in the air when they are ionized by the charged particles in the shower. Examples of experiments using this technique are Fly's Eye and Hires. The amount of fluorescent light produced by the shower is proportional to the energy of the particle initiating the shower. However, to measure the energy of the shower correctly, corrections must be made to account for the attenuation of light in the atmosphere, and the experiment can only run during moonless clear nights, which reduces the duty cycle of such experiments to 10%.

Another technique to measure the energy of the cosmic rays relies on the fact that the charged particle density in the shower sufficiently far from the shower core is proportional to the energy of the primary particle. Examples of experiments using this technique are AGASA, which uses scintillators to detect the passage of a charged particle; and Haverah Park, which uses Cherenkov light produced by the passage of charged particles in water for their detection. This technique, however, is more sensitive to the shower simulation. Since the detectors used in this technique can be made light tight, they are unaffected by ambient light conditions, and as a result, experiments using this technique have a 100% duty cycle.

Obviously, accurate energy calibration is most important in order to unambiguously establish the existence of cosmic rays at energies beyond the GZK cutoff. Either technique mentioned above, if used by itself, may have uncertainties in the energy measurement which might not be easily estimated.

The Pierre Auger Cosmic Ray Observatory is a hybrid detector, using both techniques for independent measurements of the shower energy. It will have three fluorescence detectors, overlooking a surface array of over 1,657 water Cherenkov detectors. A major strength of the Auger project lies in its ability to measure the energy of cosmic ray showers using two independent techniques which can be used for cross calibration. A detailed description of the experiment can be found in the Auger Technical Design Report.

The detector in the surface array is a water tank of 3m diameter, and is 1.2m deep. Three 8" PMT's are mounted symmetrically on the top of each tank, looking downward. Cherenkov photons produced in water by air showers are diffused by the Tyvek Sheet attached on the inner wall of the tank, and are eventually detected by the PMT's, if not absorbed by water.

Since fluorescence detectors can operate only during moon-less clear nights, their duty cycle is only ~10%. The surface detectors, however, are not affected by the ambient light, so that they can operate continuously. As a result, majority of the data from the experiment will be collected by the surface detectors. Understanding the energy calibration of the surface detectors is, therefore, particularly important, which requires us to study the PMTs and associated electronics to be used in the surface detectors carefully, and to optimize their design/operating conditions.

Different groups [1,2,3,4] within the Auger collaboration have studied PMT's for the experiment, most detailed study so far being from Penn State University [1]. However, a precise and quantitative measurement of some important characteristics of the PMT's such as linearity, Quantum Efficiency, single photoelectron spectra, and the *dark-current* behavior as a function of HV are necessary in order to compare different PMT's and select the most suitable candidate. This write up describes several measurements done on three candidate PMT's with a view to determine the most suitable PMT for the experiment.

1.2 Requirement for Surface Detector PMT's

As mentioned before, the surface detector array consists of 1,657 water tanks. Each tank is viewed by three PMT's, requiring over 5,000 PMT's to be tested and installed. The PMT's should generally satisfy the following specifications:

- Operation at low gain, approximately at 10^5 . The operating gain is determined by the largest signal we wish to observe. According to the simulations done by IPN-Orsey group, if a 10^{21} eV proton hits 500m from a tank, then a PMT produces a 300 nA *cathode current* (corresponding to approximately 2,000 photoelectrons per ns) . If the PMT is operated at a gain of 10^5 , this would result in a peak anode current of 30 mA. As a result, we can not operate the PMT's at much higher gains, since the anode current will become very large, and even the best designed PMT's (of the type under consideration) are linear only up to 100 mA of peak anode current.
- From the discussion in the above paragraph, a 10^{21} eV shower would nominally yield a peak anode current of 30 mA. However, in order to have a safety margin, we would like the PMT to be linear within 5% up to anode currents of 50 mA, at a gain of $\sim 10^5$. Since the PMT's under consideration were designed for high gain ($\sim 10^7$) operation, we will see that maintaining their linearity at low gains might require some modifications in the PMT design.
- Dark pulse rate < 10 KHz. The counting rate in tank from low energy cosmic rays alone is of the order of 10 KHz. Any dark pulse rate below this level is, therefore, acceptable.
- After pulse (in the interval 200ns-5000ns after the main pulse) ratio <5% (per incident photoelectron). A typical high-energy shower has a time spread of about 5000 ns, which necessitates a gate width of 5000 ns for digitization. Since the afterpulse is correlated with main pulse, a large afterpulse will degrade the energy resolution of the detector. If the pulse shape of the MIP signal used of calibration, and the pulse shape of a an EM shower were the same, the effect of afterpulse would cancel out to first order. However, the two signals have distinct pulse shapes, so that the cancellation is not perfect. As a result, low afterpulse probability is desirable.
- Transit time spread (TTS) <10 ns, and pulse rise time <10 ns.
- Immunity to earth's magnetic field. The candidate PMT's have a relatively large (>10 cm) distance between the photocathode and the first dynode. Also, because of the relatively large area of the photocathode, the trajectories of individual photoelectrons vary significantly depending on the position of the incident photon. As a result, any significant sensitivity to magnetic field might cause non-uniformity across the photocathode on a given PMT, and also from PMT to PMT.
- Long term reliability for ~ 20 years.

In order to find the most suitable candidate for the Auger project, we need to measure the above-mentioned characteristics for the three different kinds of PMT's under consideration. The UCLA group has set up facilities to measure all these characteristics. The measurement techniques, setup, and the results are described below.

2. Measurements

UCLA high-energy group has a long history of developing, testing and procuring photomultipliers for various high-energy experiments. We have recently modified the existing systems, which were originally developed for testing 1.5" PMT's for the KTeV CsI Calorimeter. Our testing stations include the following:

1. Quantum Efficiency
2. Gain and dark current as a function of HV.
3. Single photoelectron distributions.
4. Linearity.
5. Dark pulse rate.

6. After pulse ratio.

The following sections describe the measurements in detail.

2.1 Quantum Efficiency

2.1.1 System Setup

The quantum efficiency (QE) system at UCLA is designed to measure the photocathode current of two PMT's simultaneously at a given wavelength. One of these tubes has known quantum efficiency, used as reference to measure the QE of the other PMT.

Figures 2.1.1a and 2.1.1b illustrate how the system works. First, the light from an Oriel model 6291 Xe arc lamp set in an Oriel model 7340 housing (with a necessary ozone eater, model 66087), passes through a slit with an opening of 0.12 mm. The Xe lamp is powered by an Oriel model 68806 power supply run at 7-8 amps of current. After the slit, the light enters a monochromator (Oriel 77250) where the diffraction grating can be rotated so as to choose a wavelength. Next, the light, at the chosen wavelength, passes through another slit set at 0.12 mm and then a 50/50 splitter before it enters an integrating sphere. The 50/50 splitter is there to send light to an Oriel PMT model 7060 (powered by the Oriel 7070 photomultiplier detection system) to monitor the stability of the light source. The integrating sphere then distributes the light equally throughout the sphere so that the number of photons hitting the photocathodes of the two PMT's is equal. Also, there are identical 1-1/4" diameter openings on two diametrically opposite sides of the sphere and the PMT's are placed so that these openings are at the center of the photocathodes. The DAQ system is a LabVIEW program that uses a GPIB interface with a Keithley 486 picoammeter as well as two Stanford Research Systems PS325 high voltage supplies. This system measures the cathode currents of the two PMT's along with controlling the voltages to both of them. In order to measure the cathode current, the PMT's are operated at positive voltage, with a special base. A positive voltage of approximately 150V is applied to the first dynode, and all other dynodes are short-circuited to the first dynode. A picoammeter is connected between the photocathode and the ground. As the light hits the photocathode, electrons are emitted and are collected at the first dynode. Since the light source is continuous, a DC current flows between the photocathode and the first dynode, which is measured by the picoammeter.

Since both the PMT's are exposed to the same number of photons at the same wavelength, if the QE of one of the PMT's (the reference PMT) is known, we can obtain the QE of the other PMT by comparing the cathode currents:

$$QE_{unknown} = QE_{ref} \times \frac{I_{unknown}}{I_{ref}}$$

Where QE_{ref} is the known quantum efficiency of the reference PMT, I_{ref} is the cathode current from the reference PMT, and $I_{unknown}$ is the cathode current from the PMT to be measured.

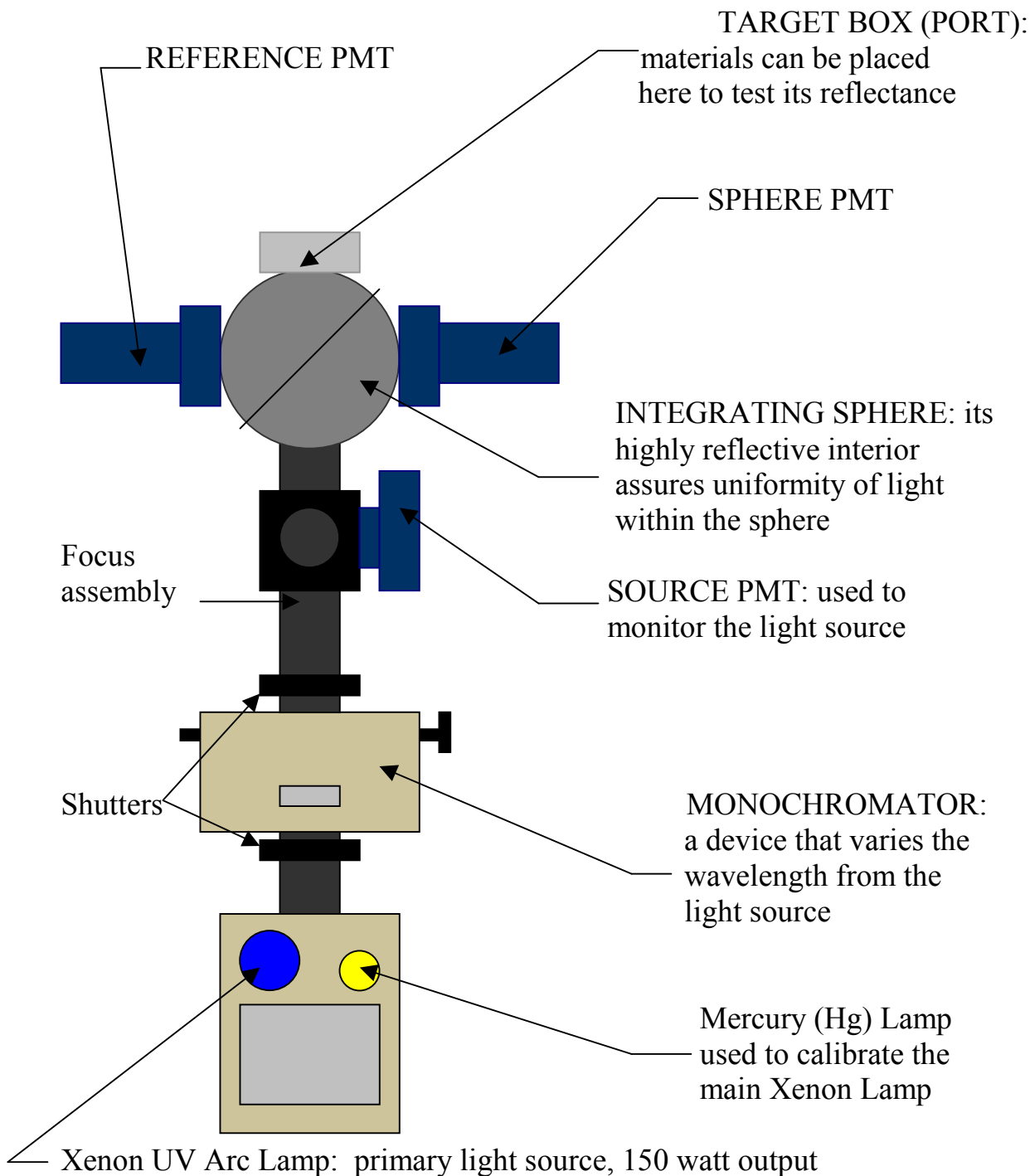


Figure 2.1.1a - The Quantum Efficiency System setup.

The monochromator makes it possible to scan multiple wavelengths and therefore to measure the quantum efficiency as a function of wavelength. The shutters make it possible to stop the light from entering the integrating sphere and slits with variable width control the amount of light that reaches the photocathodes.

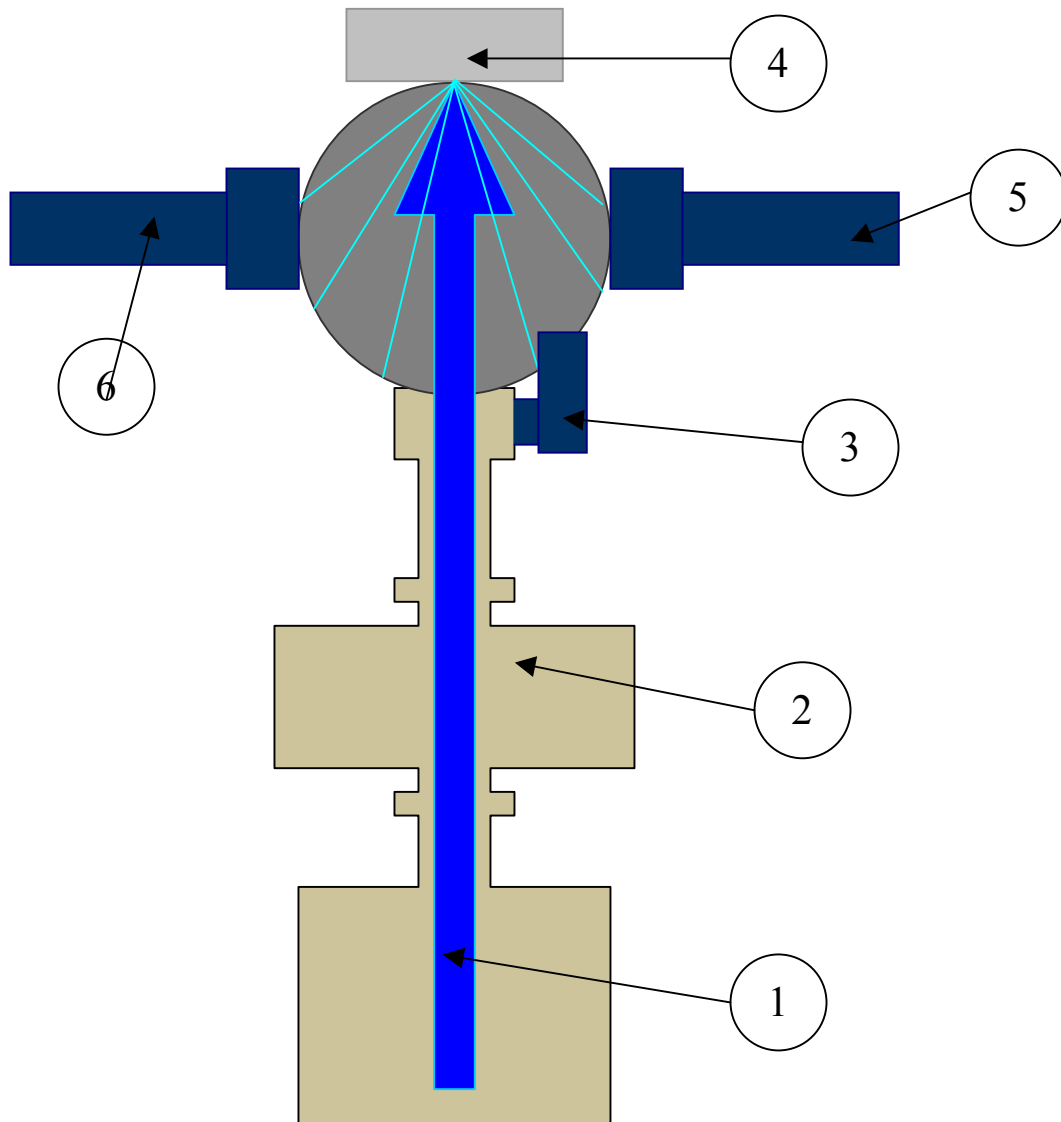


Figure 2.1.1b - A schematic of how the Quantum Efficiency System works

- (1) The Xenon lamp emits light.
- (2) The Monochromator varies the wavelength of light entering the sphere.
- (3) The Source PMT monitors the light to detect any anomalies.
- (4) The light hits the Target Box and is uniformly scattered throughout the sphere, causing the two PMT's to be exposed to equal amounts of light flux.
- (5) Cathode current from the unknown PMT is compared with that from the reference PMT to calculate the QE.

2.1.2 Data Taking and Results

The goal was to measure the quantum efficiency (QE) of the six different PMT's from three different companies. The QE was measured at varying wavelengths, from 280 nm to 700 nm in 20 nm steps to see the characteristic QE graph for each company.

A Hamamatsu R6234 hexagonal PMT (serial number SR9390) was used as reference because its QE was known, the measurements being provided by the company. We chose the HV applied to the first dynode, and the incident light intensity to ensure the accuracy of our results in the following manner.

First, for a constant light intensity, cathode current varies with the dynode voltage. At low voltages, the cathode current increases linearly with the applied voltage, because the efficiency of the first dynode to collect the photoelectrons increases. At higher voltages, however, the first dynode reaches its maximum photoelectron collection efficiency, and therefore the cathode current levels off and reaches a plateau. We wish to operate in this plateau region. Results for the six test PMT's are presented in figures 2.1.2a, and based on these results we used 150 volts as the high voltage supplied to the tubes.

Second, at a constant voltage, cathode current and light intensity have a linear relationship for low intensities. If, however, the light intensity is too high, the relationship ceases to be linear due to resistivity of the photocathode. We desire to operate in the linear region. The cathode current as function of incident light intensity was measured for the six test PMT's and the results are plotted in figures 2.1.2b. The operating intensity is definitely in the linear region, corresponding to a source PMT voltage of around 0.7-0.8 volts, or a current of 7-8 amps supplied to the lamp.

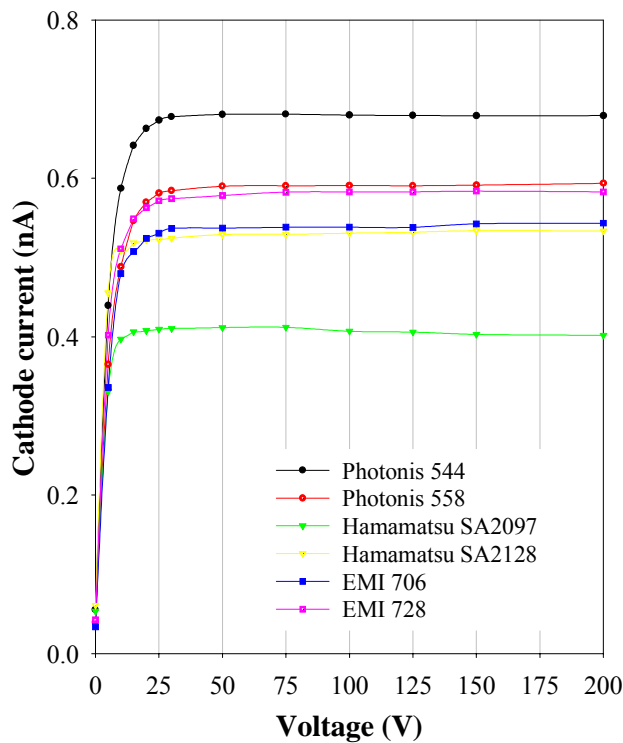


Figure 2.1.2a - Cathode current vs. dynode voltage.

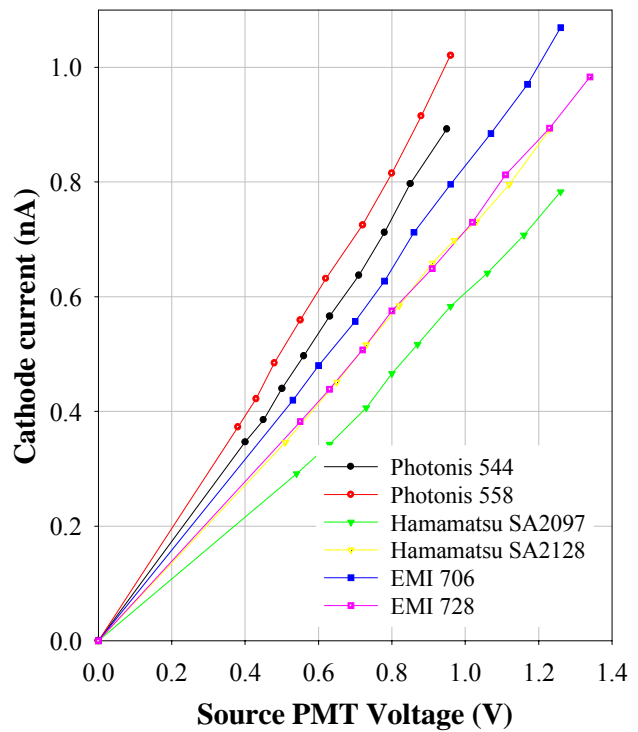


Figure 2.1.2b - Cathode current vs. source PMT pulse height (which is proportional to the incident light intensity).

These same measurements were made for the Hamamatsu R6234 reference tube as well. The results are shown in figures 2.1.2c,d.

Hamamatsu R6234

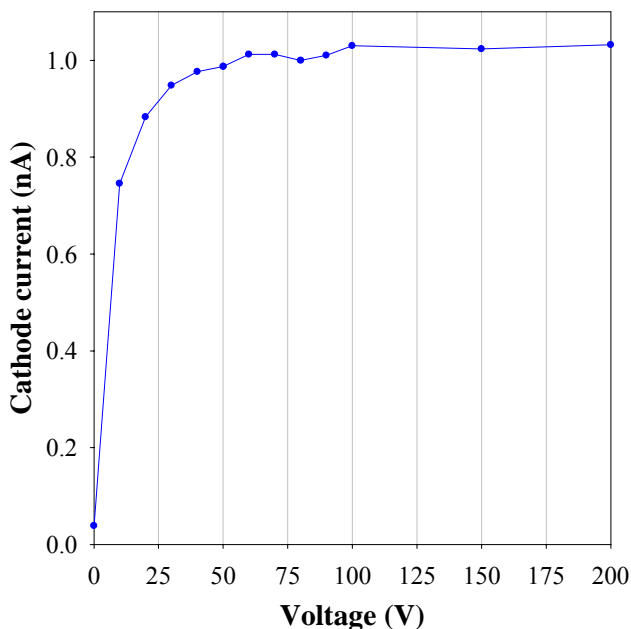


Figure 2.1.2c Cathode current vs. dynode voltage for the reference PMT.

Hamamtsu R6234

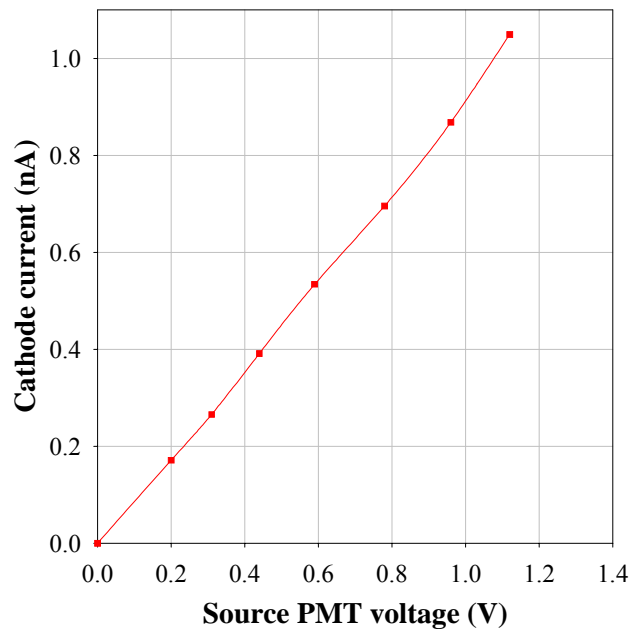


Figure 2.1.2d Cathode current vs. source PMT pulse height (which is proportional to the incident light intensity).

Now, knowing that these potential error-causing problems are taken care of, data can be taken for the different tubes. Initial measurements were taken and then repeated several days later to guarantee the accuracy of the data. To make the measurements the following process was used: First, high voltage was supplied to both PMT's, with no light being let in, and the cathode dark current was measured. Next, light from the Xe lamp was allowed to enter into the sphere and the wavelength of light was varied using the monochromator. At each wavelength the cathode current for both PMT's was measured. The cathode dark current was subtracted from these measurements. Then the QE was calculated, as mentioned above.

To detect any systematic error in the method, the QE system was used to measure the QE of another hexagonal tube, Hamamatsu R6234-SR9336, whose QE is also known. As can be seen in figure 2.1.2e, our measurement agrees well with the measurements provided by the company. The results for the six test PMT's can be seen in figures 2.1.2f-i.

2.1.3 Discussion

Our measurements of the QE for the three different kinds of PMT's are shown in Figures 2.1.2f-i. EMI 9353KB has the highest characteristic peak quantum efficiency of 25-28% at 360 nm. These tubes also showed the highest quantum efficiency in the range of 350-400 nm. The Hamamatsu R5912 and Photonis XP1802 tubes had peak quantum efficiencies of 21-24% each. Their peak efficiency was also around 360 nm. There is an interesting feature of the EMI 9353KB tube serial number 728; its quantum efficiency is significantly larger at 300 nm than any other phototube, around 19%. The company accounted for this by saying it is possible that the material of the glass bulb for this PMT is different than the other phototubes, thereby resulting in higher quantum efficiency at ultra-violet wavelengths.

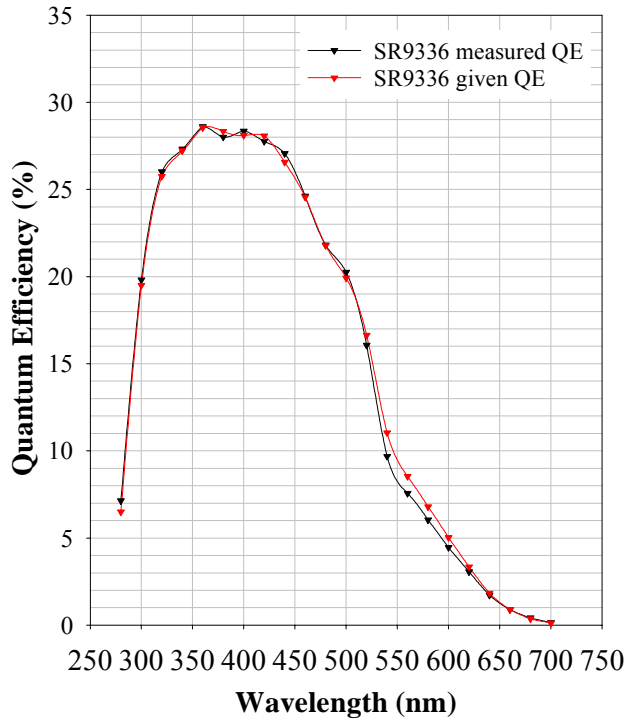


Figure 2.1.2e – Measured and actual Quantum efficiencies as a function of wavelength for Hamamatsu R6234-SR9336.

EMI 9353KB

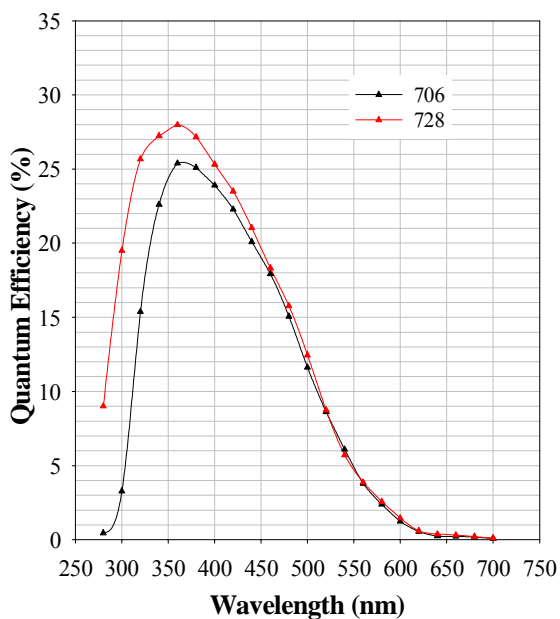


Figure 2.1.2f - Quantum efficiency as a function of wavelength for EMI 9353KB.

Hamamatsu R5912

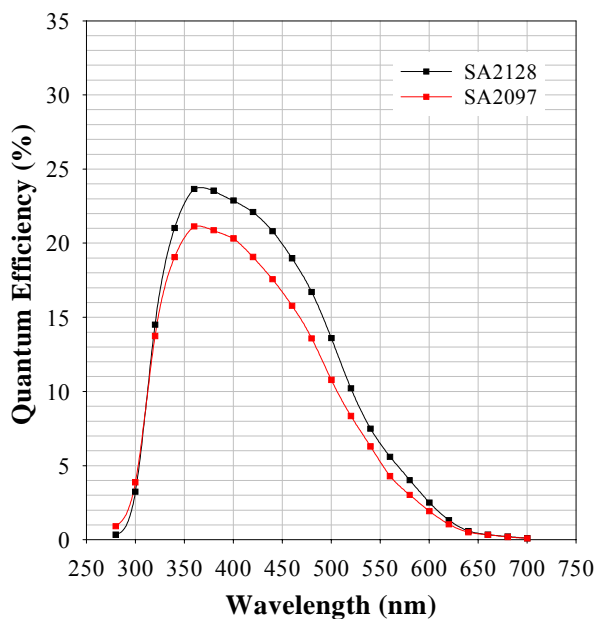


Figure 2.1.2g - Quantum efficiency as a function of wavelength for Hamamatsu R5912.

Photonis XP1802

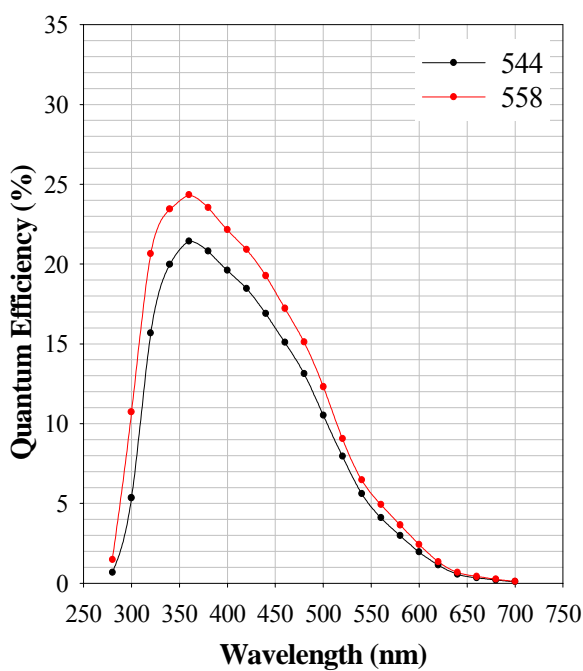


Figure 2.1.2h - Quantum efficiency as a function of wavelength for Photonis XP1802.

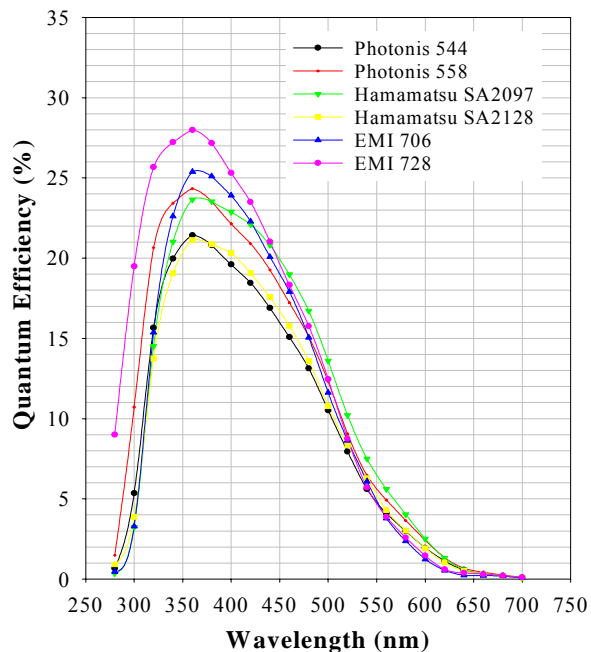


Figure 2.1.2i - Quantum efficiency for all PMT's.

2.2 Gain and Dark Current

We have measured absolute gain and dark current curves for each PMT. The system setup, method and the results are described in this section.

2.2.1 Absolute Gain Measurement by Single PE Peak

We obtained the absolute gain for each PMT by measuring the single photoelectron peak. A pico-second laser (Hamamtsu PLP-01) was used as a light source, which also provides a NIM trigger output that was used to generate the gate for the ADC. The DAQ system is LabView based. A continuously variable filter wheel, placed between the laser and the PMT, allowed us to control the intensity of light reaching the PMT. The PMT was allowed to calm down for 30 minutes under high voltage in the dark box before making the measurements. A schematic of this setup is shown in Figure 2.2.1a.

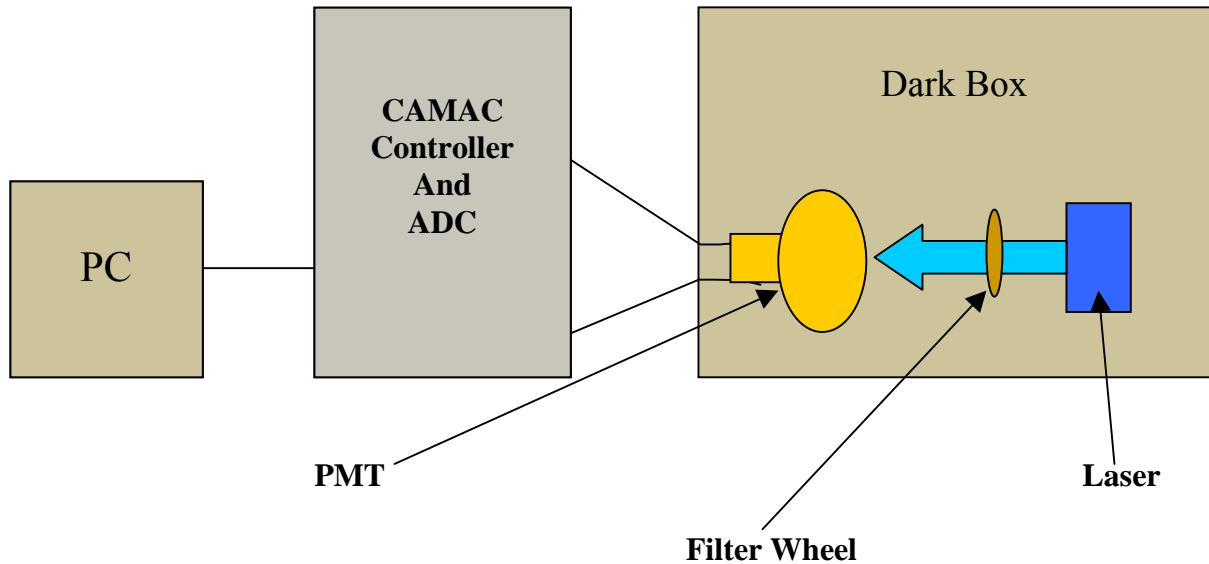


Figure 2.2.1a - Schematic of the setup used for measuring single photoelectron peaks.

The voltage dividers used for these measurements, as well as dark current and linearity measurements are described in Appendix A. These are tapered-bleeder voltage dividers, designed for high linearity under pulsed operation. Positive HV base was used to measure the single photoelectron peaks and linearity for the EMI PMT's only. Negative HV bases were used for all other PMT's.

First we apply a high voltage to the PMT to ensure an approximate gain of over 10^7 . Then we reduce the intensity of the light incident on the PMT to a level such that approximately 90% of the time we get pedestal readings from the ADC (pedestal was contained in one ADC channel and was stable). This ensures that any signal seen above pedestal is mostly from single photoelectrons. From Poisson statistics,

$$P(n) = \frac{e^{-\mu} \mu^n}{n!}$$

Where $P(n)$ is the probability of observing exactly n photoelectrons within the gate in one laser pulse, with μ photoelectrons reaching the first dynode per pulse on an average. Since the intensity of light reaching the PMT is such that 90% of the time no signal is observed, the probability of seeing no

PE is $P(0) = e^{-\mu} = 0.9$, so that $\mu = 0.105$. The probability of seeing a single PE is, then $P(1) = \mu e^{-\mu} = 0.095$. Therefore, $P(n > 1) = 1 - 0.9 - 0.095 = 0.005$. Consequently, any signal observed above pedestal is dominated by single PE events, since $P(n=1)/P(n>1) = 21$.

Once we have the single photoelectron peak from a PMT, absolute gain at that High Voltage is known. The single PE spectra of the different PMT's are shown in Figures 2.2.1b-d. Hamamtsu R5912 PMT's have the best resolution for detecting single photoelectrons, with the highest value of peak-to-valley ratio. The Photonis XP1802/FLB PMT's have the worst peak-to-valley ratio for the single PE peak.

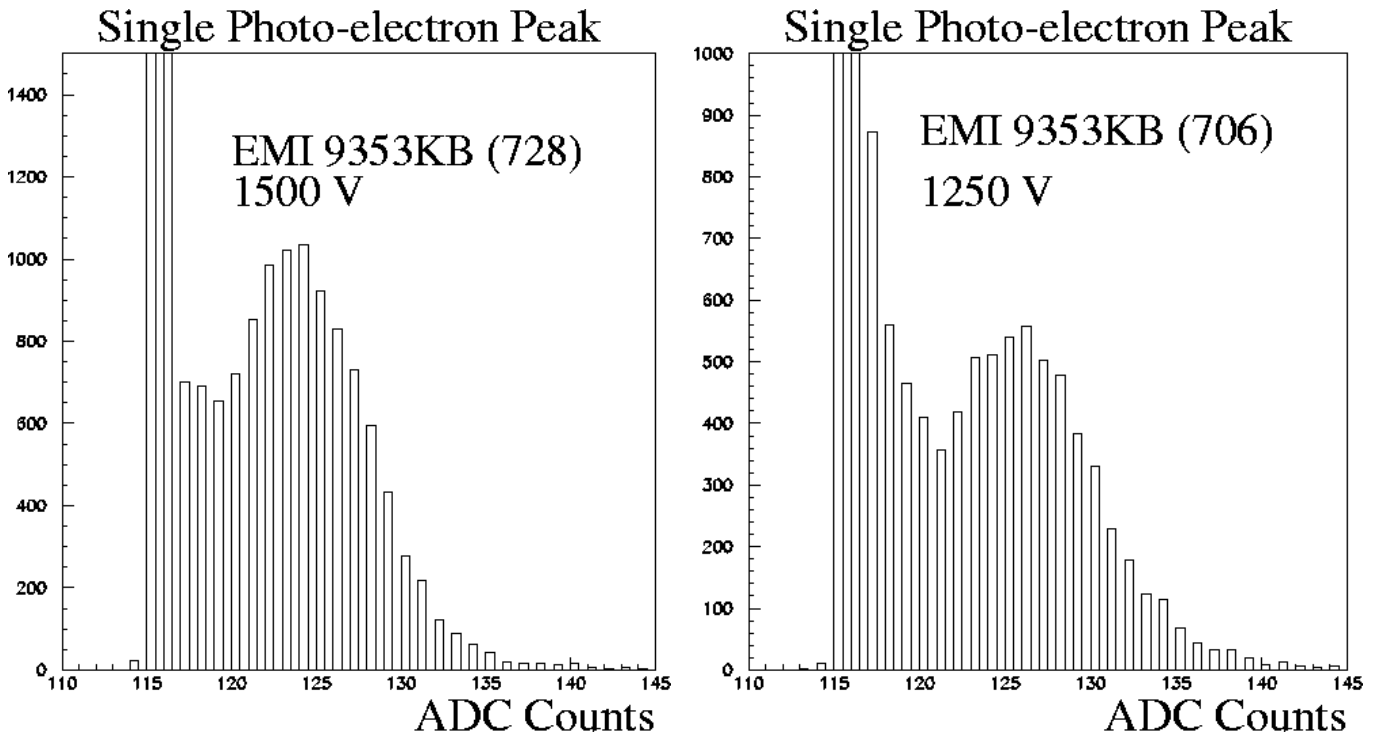


Figure 2.2.1b - Single photoelectron spectra from the two EMI 9353KB PMT's.

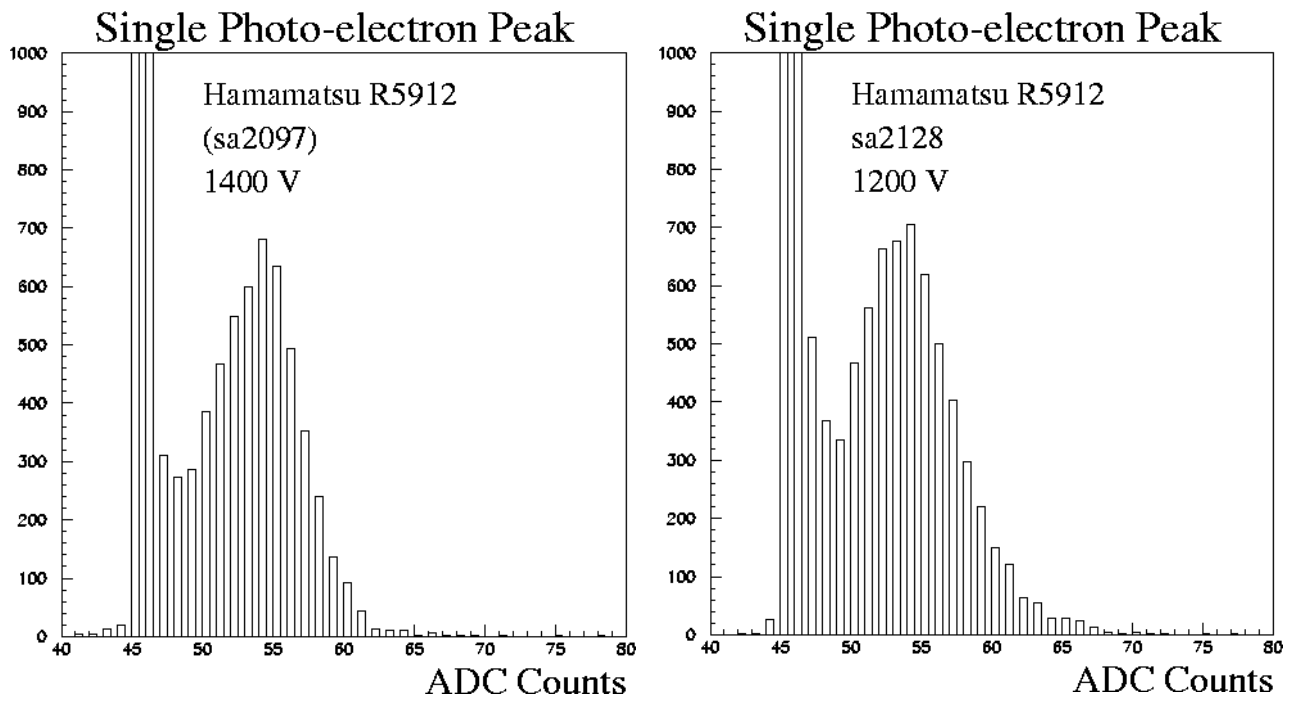


Figure 2.2.1c - Single photoelectron spectra from the two Hamamatsu R5912 PMT's.

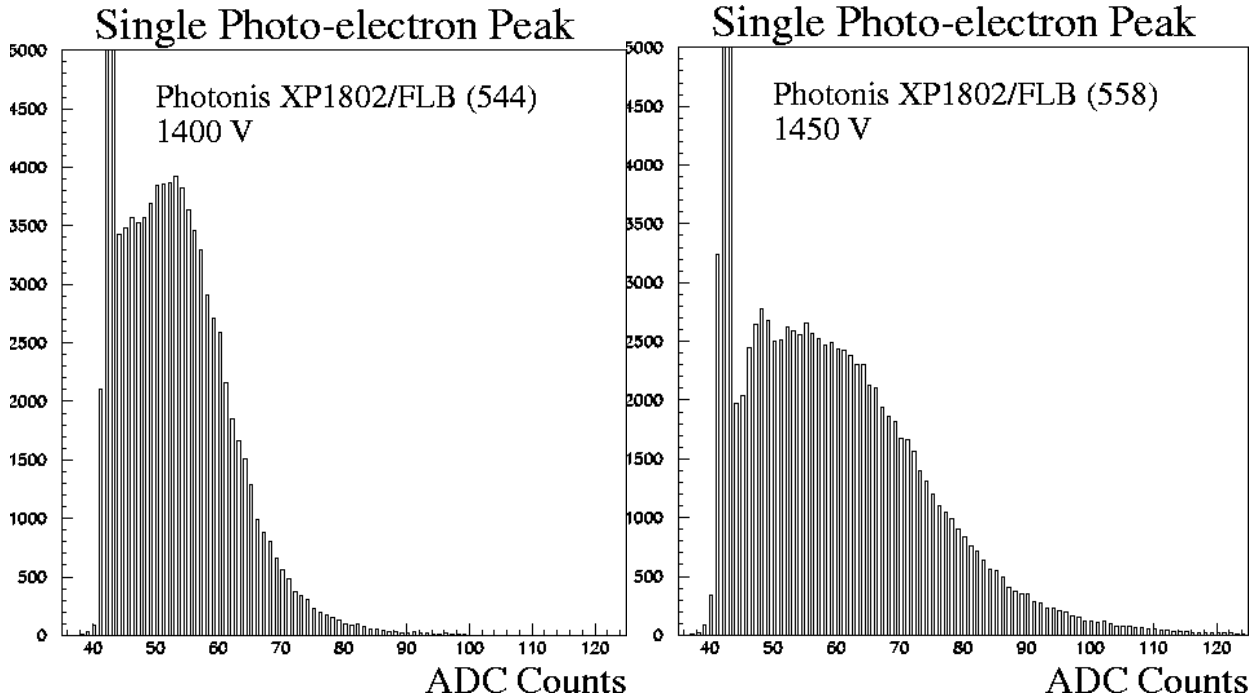


Figure 2.2.1d - Single photoelectron spectra from the two Photonis XP1802/FLB PMT's.

2.2.2 Dark Current and DC Gain measurement

Once we know the absolute gain of a PMT at a given voltage from the single PE peak, we can obtain the gain curve by measuring the anode current (after dark-current subtraction) as a function of high voltage for a constant flux of light incident on the PMT.

Both dark current and DC gain are measured using the setup in figure 2.2.2a. A deuterium lamp (Oriel) was used as a continuous light source. Filters allow us to control the intensity of light incident on the PMT, and shutters allow us to block the light from reaching the PMT for dark current measurements. The anode current was measured using a Keithley 486 picoammeter, and the whole measurement system was automated using Lab View software and GPIB interface.

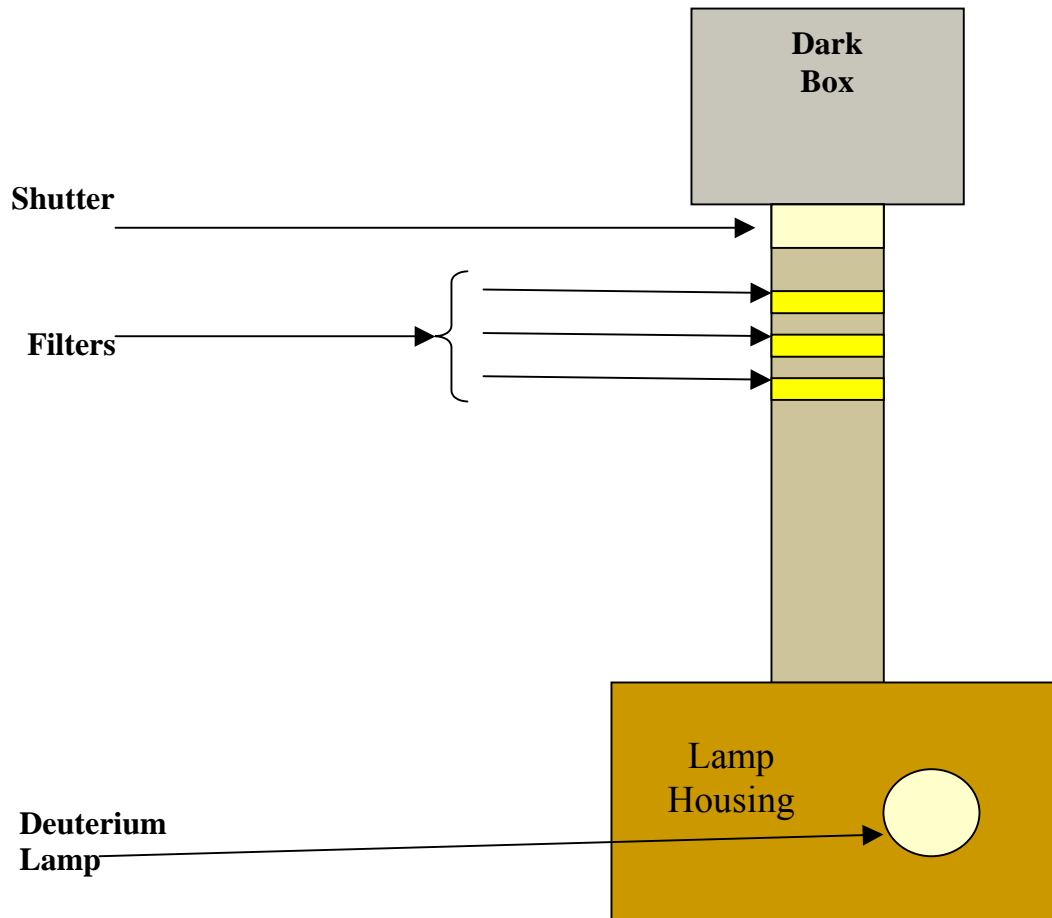


Figure 2.2.2a Schematic of the setup used to measure dark current and DC gain.

Dark current is the current that flows between the anode and the photocathode even when there is no light incident on the PMT. It is caused mainly by the leakage current, thermionic emission, field emission and background radiation. The dark current also depends on the length of time the PMT has been stored in dark. Therefore, we have to allow the PMT's to settle down in dark for a sufficiently long period before any meaningful measurements can be made.

First, we studied the behavior of the dark current as a function of storage time in dark. The PMT's were briefly exposed to the ambient light in the lab, and then they were put back in the dark box, and the dark current at 1500V was measured as a function of storage time in dark. The results of these measurements are shown in figures 2.2.2b-d. Clearly, all PMT's have a very large dark current

immediately after exposure to light. However, the dark current falls rapidly to less than 100 nA after 30 minutes storage in dark.

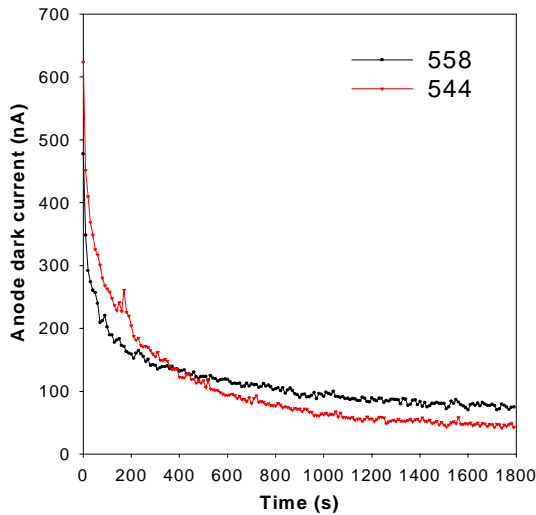


Figure 2.2.2b - Dark current as a function of storage time in dark for Photonis XP1802 at 1500V.

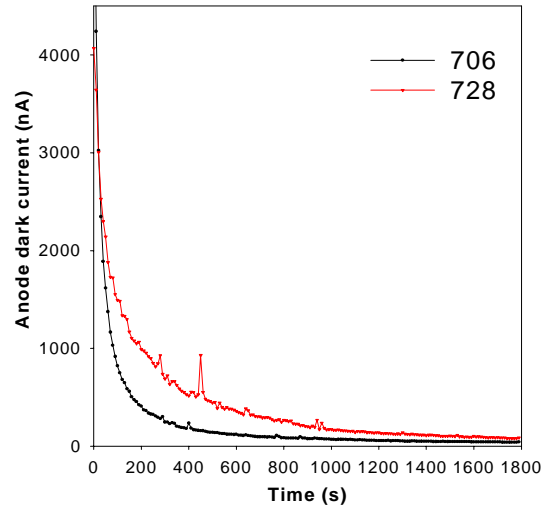


Figure 2.2.2c - Dark current as a function of storage time in dark for EMI 9353KB at 1500V.

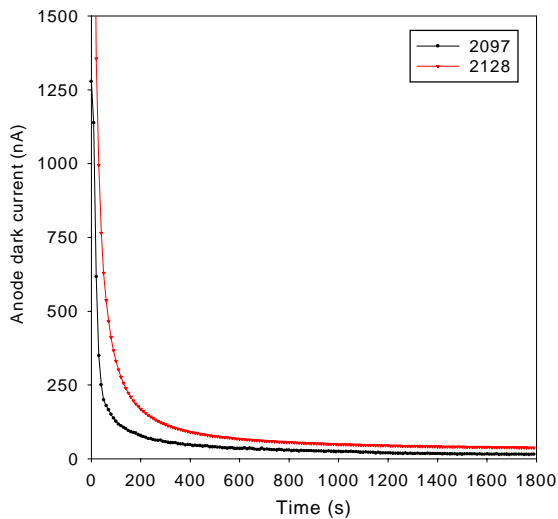


Figure 2.2.2d - Dark current as a function of storage time in dark for Hamamatsu R5912 at 1500V.

DC gain was obtained by measuring the anode current as a function of HV for a given constant flux of light incident on the PMT. For accurate gain measurements the intensity of the light incident on the PMT was adjusted such that the anode current for each tube was 100 times the dark current and 1% of the bleeder current of the base. The HV to the PMT was changed in 200V increments, and the corresponding anode current, and the dark current was measured.

The gain obtained by this method is only relative, because the absolute intensity of the incident light is not known. The normalization of this gain curve was fixed by the absolute gain obtained from the single PE method at a given voltage.

2.2.4 Data Taking and Result

Results for the EMI phototubes are seen in figures 2.2.4a and 2.2.4b. The slopes of the gain and dark current curves are parallel for voltages between 1000 and 2000 volts. For PMT 9353-728, the trend indicates that they might stay parallel for even higher voltages. At voltages of 1000 volts or lower, the dark current plots level off horizontally, indicating it is dominated by electronic noise at low gains.

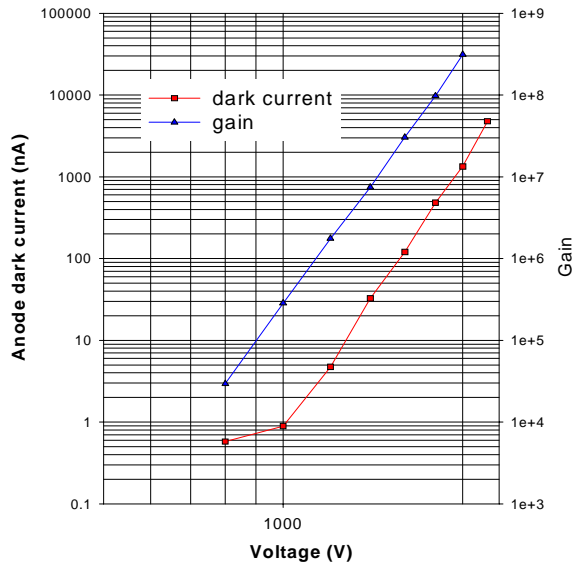


Figure 2.2.4a Dark current and gain for EMI 9353KB-728

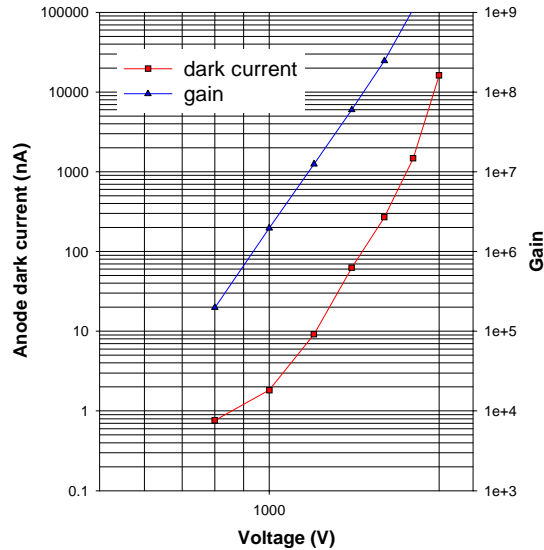


Figure 2.2.4b Dark current and gain for EMI 9353KB-706

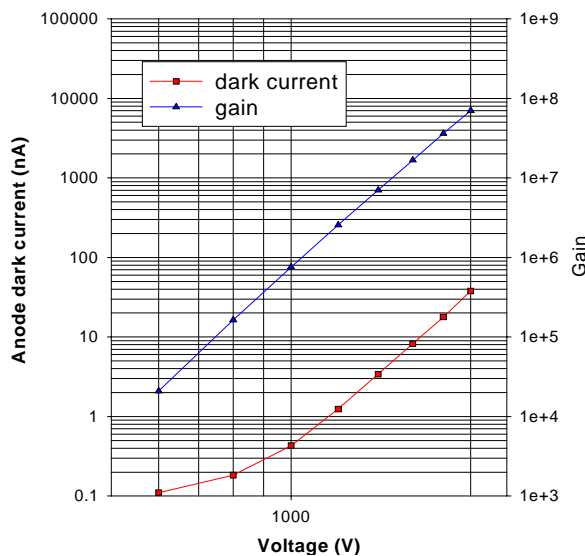


Figure 2.2.4c Dark current and gain for Hamamatsu R5912-sa2128

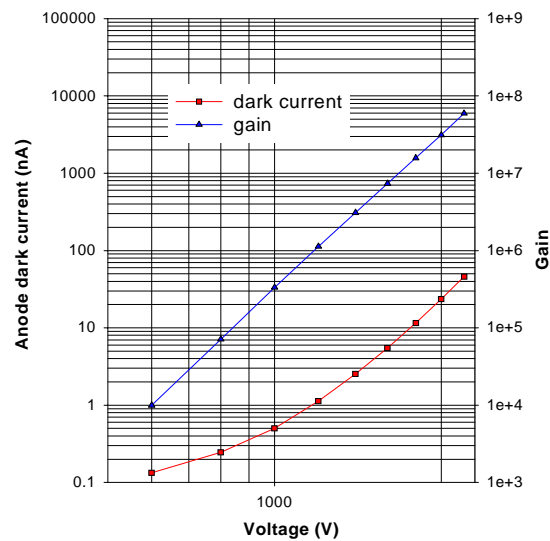


Figure 2.2.4d Dark current and gain for Hamamatsu R5912-sa2097

Data for Hamamatsu R5912 PMT's is shown in figures 2.2.4c-d. Both PMT's appear to be stable beyond the highest voltage used for these measurements. Again at lower voltages, below 1000 volts, the dark current becomes dominated by electronic noise and is no longer parallel to the gain curve.

The results for the Photonis PMT's are shown in figures 2.2.4e-f. The range of voltages where the dark current curve is parallel to the gain curve appears to be smaller than both Hamamatsu and EMI PMT's. At low voltages the characteristic flattening out of the plot due to noise is seen and at voltages above 2000 V, both PMT's become unstable.

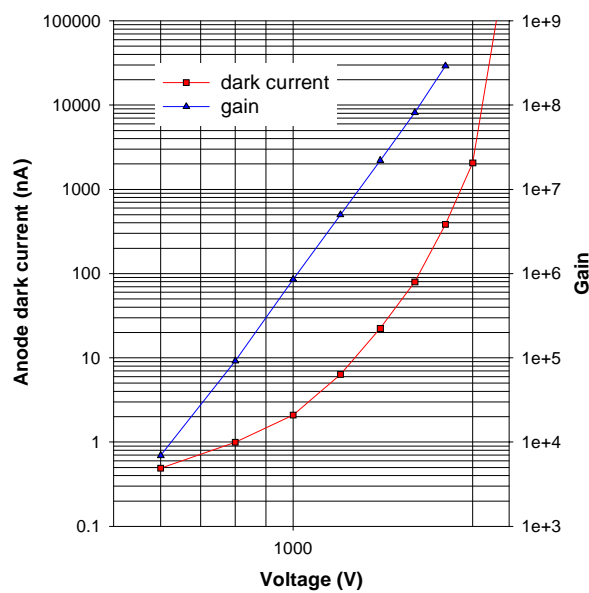


Figure 2.2.4e Dark current and gain for Photonis XP1802-544.

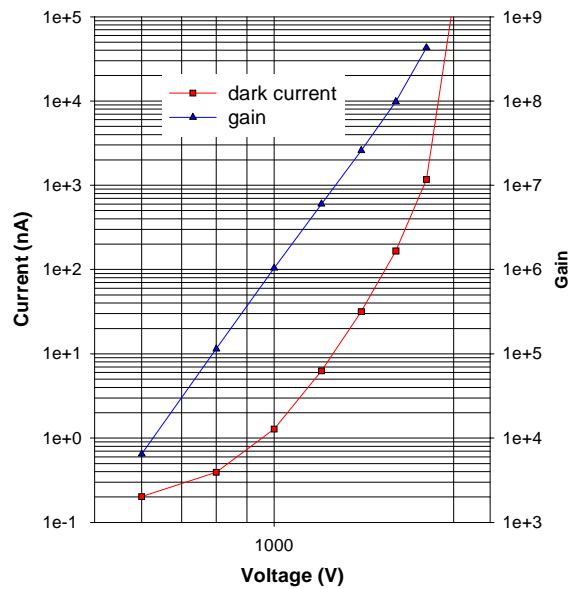


Figure 2.2.4f Dark current and gain for Photonis XP1802-558.

2.3 Linearity

As mentioned previously, the PMT's used in the Auger project will be required to detect from a MIP signal (a single muon going through the tank) to up to $\sim 10^5$ photoelectrons, corresponding to the highest energy showers. As a result, these PMT's should be linear over a wide range of anode currents, in order to measure the energy of the highest energy showers accurately. We have setup a system at UCLA to do a precise linearity measurement, and have tested three different kinds of PMT's. The setup, technique, and the results are described below.

2.3.1 System Setup

The UCLA PMT Linearity Test System has been custom-constructed to determine subject PMT linearities to better than 1% precision. Currently operational in its first-generation form, it has already exceeded expectations, allowing for measurements of linearity as good as 0.5% precision thus far. The system setup is described in detail in Appendix A.

The Linearity Test System employs successive bursts of light of varied intensity to measure the nonlinearity of the PMT as a function of peak anode current. More specifically, the system uses an LED driver to pulse two blue LED's in succession, followed by a simultaneous pulsing of the two LED's together. The charge output by a given PMT as a result of each of the three successive bursts is registered individually by a LeCroy 2249W ADC. The brightness of each LED is tuned such that one of them is brighter than the other. As a result, when they are fired in the above mentioned sequence (LED1, LED2, and LED1+LED2 simultaneously), the PMT sees a sequence of a dim light pulse, a bright light pulse, and then an even brighter light pulse, whose intensity is equal to the sum of the previous two pulses. The PMT charge output corresponding to these three different light intensities are digitized by an ADC.

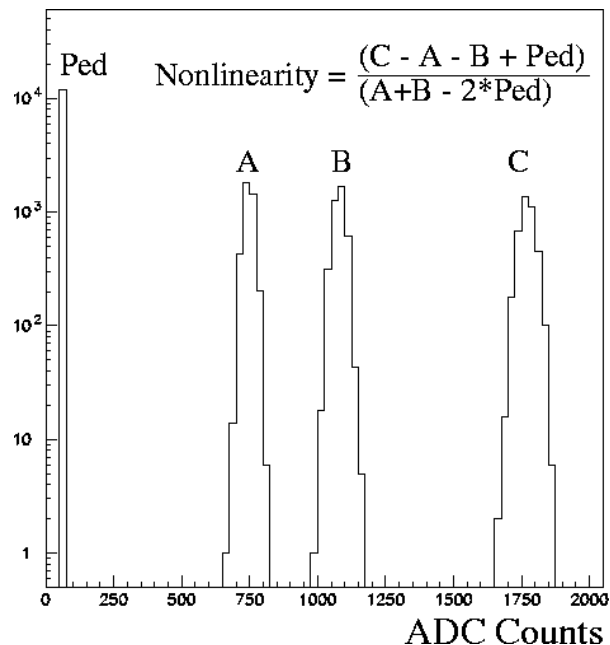


Figure 2.3.1a - A typical ADC plot of the PMT charge output obtained from the linearity system.

Figure 2.3.1a shows a typical ADC plot of the PMT charge output from the linearity system. Three distinct peaks correspond to the three different LED burst as seen by the PMT. Peak A corresponds to the dim LED pulse, peak B corresponds to the bright LED pulse, and peak C corresponds to the case when both the dim and the bright LED fire simultaneously. If the PMT is truly linear, then the position of peak C should be exactly equal to the sum of the positions of the peaks A and B (after subtracting the pedestal from all peak positions); i.e., for a linear PMT,

$$C - \text{Pedestal} = (A - \text{Pedestal}) + (B - \text{Pedestal}).$$

Any deviation from linearity is defined as:

$$\begin{aligned}
 \text{Nonlinearity} &= \frac{[(C - \text{Pedestal}) - \{(A - \text{Pedestal}) + (B - \text{Pedestal})\}]}{[(A - \text{Pedestal}) + (B - \text{Pedestal})]} \\
 &= \frac{[C - A - B + \text{Pedestal}]}{A + B - 2(\text{Pedestal})}
 \end{aligned}$$

Note that in this method of measuring the linearity, we don't need to know the absolute brightness of each LED pulse. As a result, this method is not sensitive to the changes in LED brightness over time, or the knowledge of the absolute transmittance of the filter. Consequently, systematic errors attributable to the light source are removed.

2.3.2 Data Taking and Results

In order to measure the linearity, we use the bases described in Appendix A. Positive HV base was used for EMI PMT's, while negative HV bases were used for Hamamatsu and Photonis.

A computer controlled continuous filter wheel placed in between the PMT and the LED's allows us to control the intensity of the light reaching the PMT. The PMT output is digitized using a LeCroy 2249WADC, and the peak output pulse height (and hence peak anode current) is measured using a Tektronix TDS 654C digital oscilloscope.

First, we tested the linearity system using a fine mesh PMT. These PMT's are extremely linear even at very high anode currents, because there is no space charge effect involved. Therefore, any nonlinearity observed in this PMT would be due to the intrinsic nonlinearity of the light source, or a systematic effect because of the measurement technique. Figure 2.3.2a shows the results of the linearity measurement for Hamamatsu R2490MOD fine mesh PMT. Clearly, we get a nonlinearity consistent with zero for peak anode currents of up to 100 mA. This demonstrates that there is no systematic nonlinearity introduced by the linearity system and the measurement technique itself.

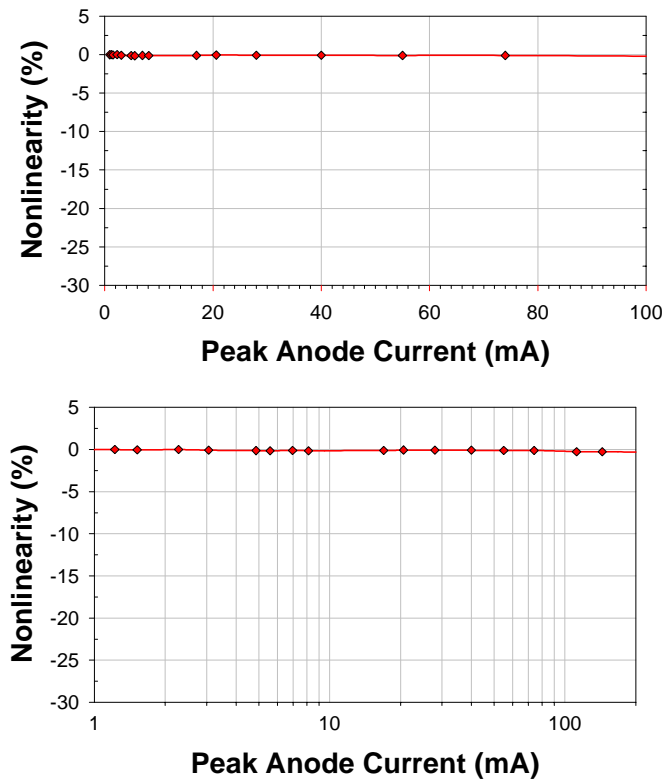


Figure 2.3.2a - Nonlinearity for R2490 Fine Mesh PMT (2200V)

The results of the nonlinearity measurements on EMI 9353, Hamamtsu R5912 and Photonis XP1802 PMT's are shown in Figures 2.3.2b, 2.3.2c and 2.3.2d respectively.

Non-Linearity EMI 9353KB-728

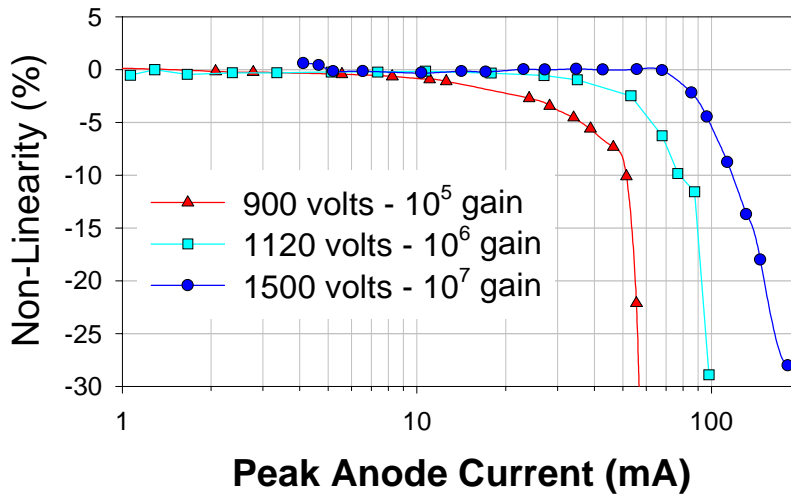
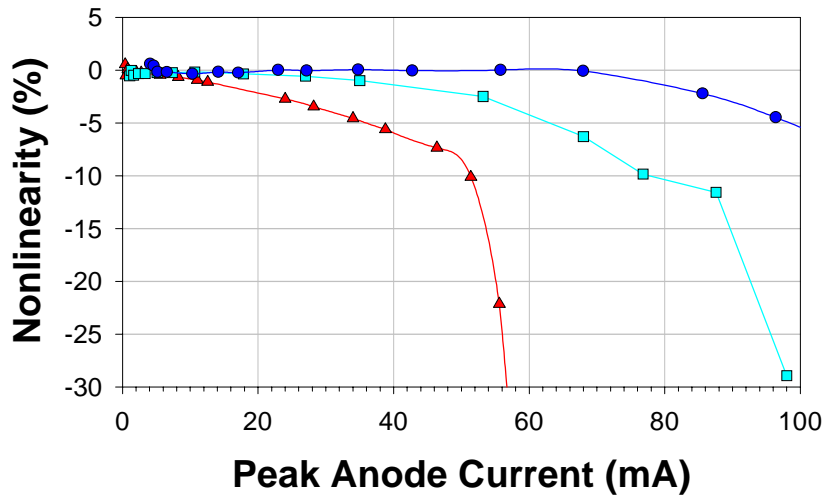


Figure 2.3.2b - Nonlinearity as a function of peak anode current for EMI 9353 PMT. The top graph shows the anode current on a linear scale, and the bottom plot on log scale.

Non-Linearity Hamamatsu R5912-SA2128

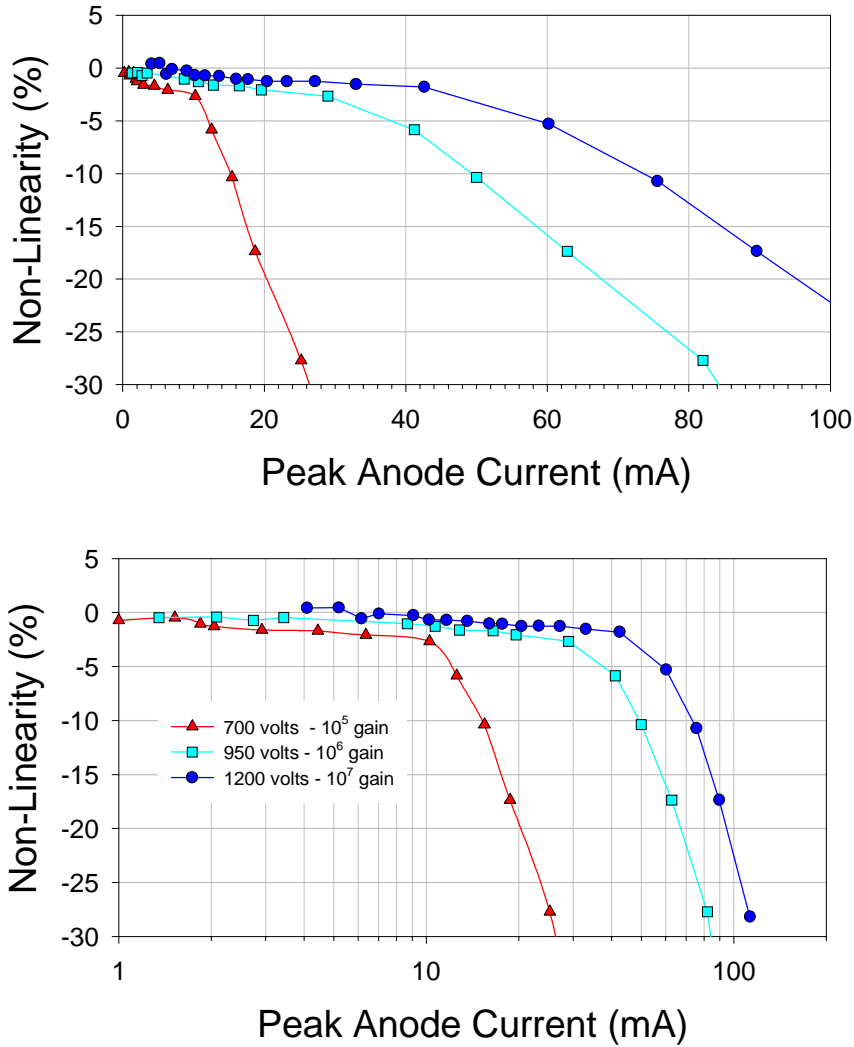


Figure 2.3.2c - Nonlinearity as a function of peak anode current for Hamamatsu R5912. The top graph shows the anode current on a linear scale, and the bottom plot on log scale.

Non-Linearity Photonis XP1802-544

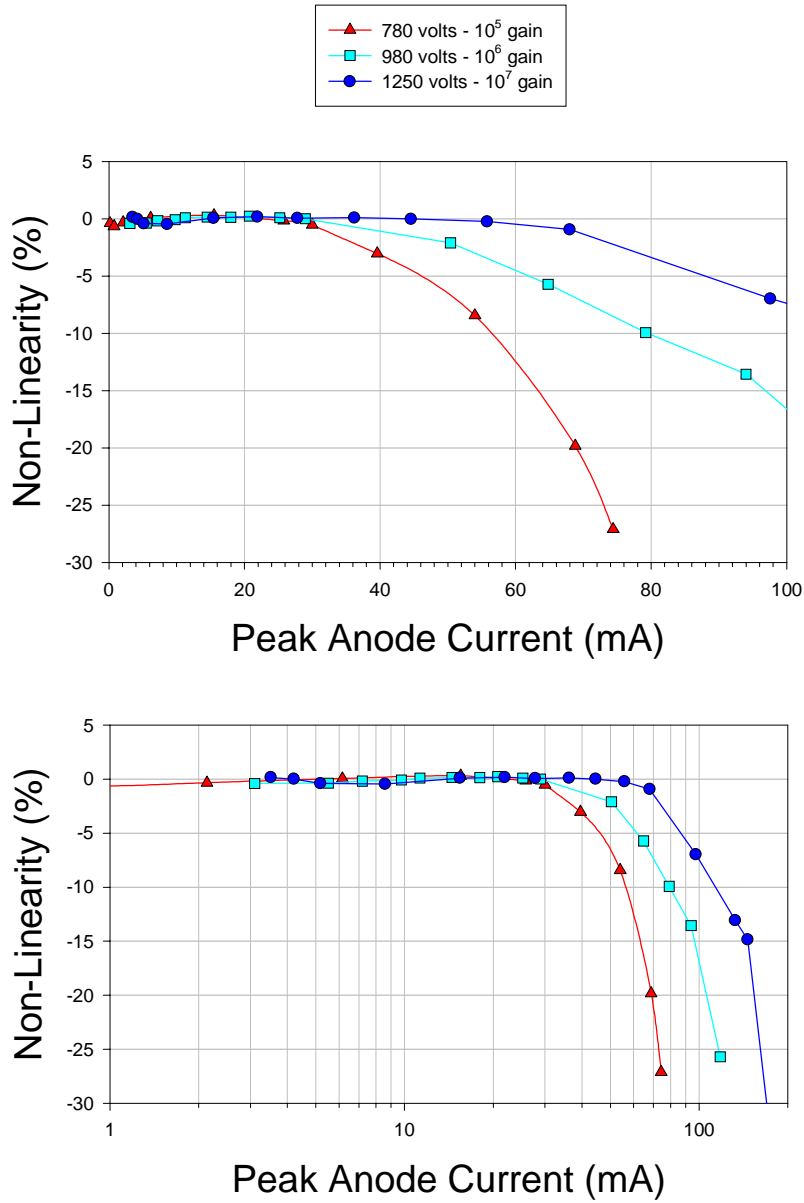


Figure 2.3.2d Nonlinearity as a function of peak anode current for Photonis XP1802/FLB. The top graph shows the anode current on a linear scale, and the bottom plot on log scale.

2.3.2 Discussion

All PMT's show a marked degradation in linearity for peak anode currents greater than 20mA when operated at low gain ($\sim 10^5$). This is expected, since there is not enough potential difference between the last dynode and the anode to overcome the space charge effect, when the PMT is operated at lower voltage. For a given gain, Photonis XP1802 exhibits the best linearity. Hamamatsu R5912 exhibits the most non-linear behavior at low gains.

2.4 Dark Pulse Rate

Dark pulses are the pulses produced by a PMT, even when there is no light incident on the photocathode. At room temperature, the dominant source of these pulses is the thermal emission of electrons from the photocathode. If the dark pulse rate is too high, it can become a significant source of background.

We have measured the dark pulse rate for each PMT as a function of storage time in dark. The high voltage for each PMT was tuned such that single photoelectron spectrum peaked at 10 ADC counts above the pedestal, which corresponds to 2.5 pC charge output. The PMT's were briefly exposed to the ambient light in the lab, then put back in the dark box. After applying the high voltage, the PMT count rates were measured at different times intervals, for two hours. Only the pulses that were 0.3 PE above pedestal were counted. The results are shown in Figures 2.4a-c.

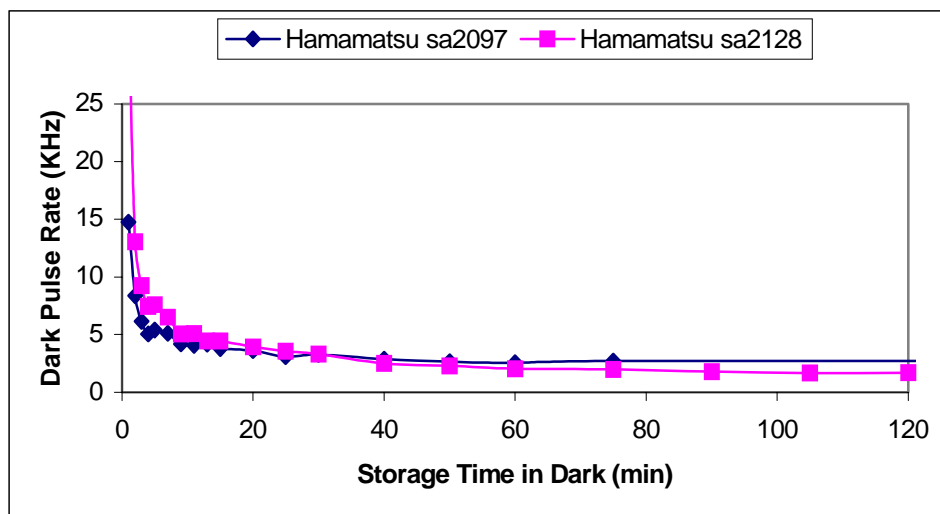


Figure 2.4a Dark pulse rate as a function of storage time in dark for Hamamatsu R5912.

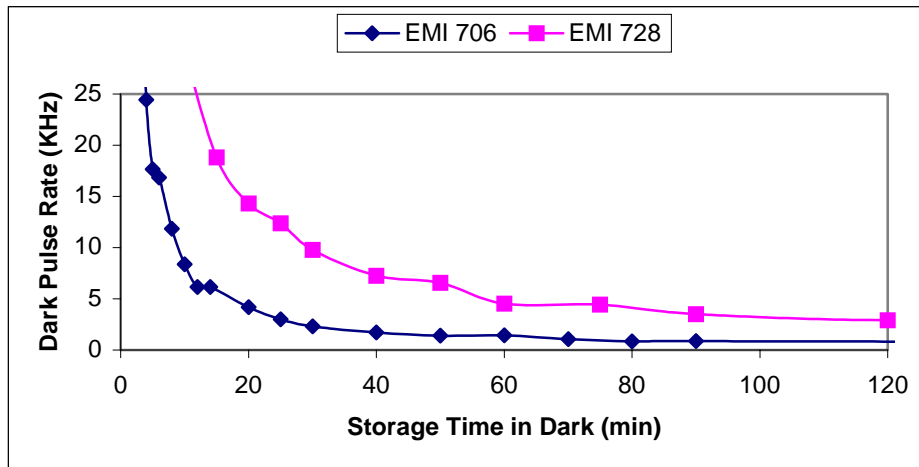


Figure 2.4b Dark pulse rate as a function of storage time in dark for EMI 9353 KB.

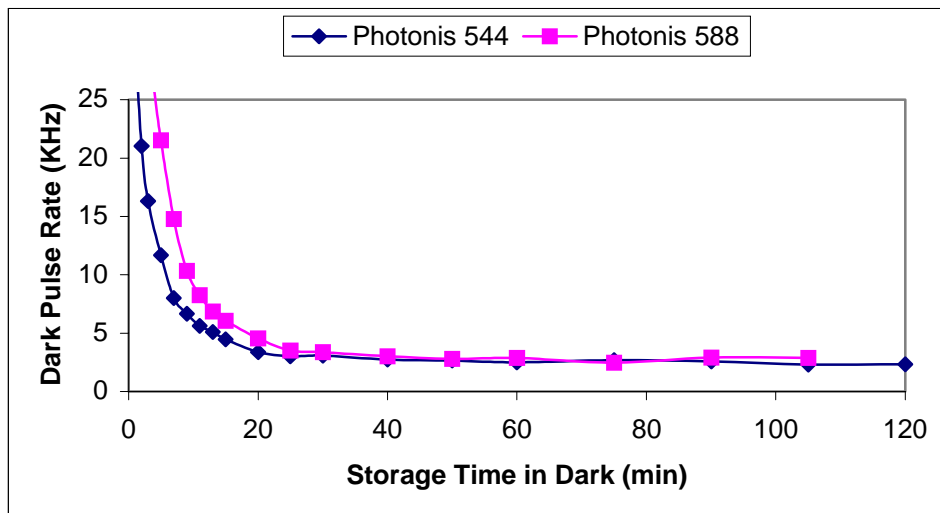


Figure 2.4c Dark pulse rate as a function of storage time in dark for Photonis XP1802.

All PMT's settle down to dark pulse rates of less than 3 KHz after storage in dark for about an hour. Since the counting rate per PMT from the low energy cosmic rays alone will be of the order of 10 KHz, dark pulse rate is not a problem for any of the PMT's.

2.5 Afterpulse Ratio

As the electrons accelerate towards the dynodes in the PMT, they can ionize residual gases in the glass bulb, or knock out ions from the dynodes. These ions, being positively charged, can hit the photocathode and cause a pulse that comes after the main pulse. The delay between the main pulse and the after pulse can be a up to a few microseconds for 8" PMT's and it depends on the mass of the ion for a given HV. The afterpulse ratio (*APR*) is defined as:

$$APR = Q_{MAIN} / Q_{AP}$$

Where Q_{MAIN} is the total charge in the main pulse, and Q_{AP} is the total charge in the afterpulse. In the Auger experiment, high energy cosmic ray showers have a time spread of approximately 5 μ s. Therefore, and afterpulses arriving within 5 μ s after the main pulse would get digitized as part of the main signal, and this will result in overestimate of the signal. Therefore, we need to measure the afterpulse ratios for all PMT's and ensure that they are within acceptable limits.

The measurement of afterpulse ratio was done using a pico second laser. First, we measured the total charge output of the PMT from the main pulse by digitizing the main pulse with a narrow gate (~40 ns). Then, for the same amount of light incident on the PMT, the charge in the late pulse was measured with a wide gate, which started 200 ns after the main pulse, and was 4800 ns wide. Therefore, the afterpulses measured here collected in a time window 200ns-5000ns after the main pulse. The results of the measurement are listed in Table 1.

PMT	Gain	Number of PE in the Main Pulse	Charge in the Main Pulse (pC)	Charge in Afterpulse (200-5000ns) (pC)	Afterpulse Ratio (%)
EMI 706	1.7×10^7	26	74.0	1.7	2.3
EMI 728	1.2×10^7	57	111.1	7.9	7.1
Hamamatsu sa2097	1.1×10^7	35	61.2	3.5	5.8
Hamamatsu sa2128	1.2×10^7	28	54.9	1.6	3.0
Photonis 544	1.6×10^7	36	93.5	4.4	4.7
Photonis 558	1.3×10^7	39	80.2	3.0	3.7

Table 1 Afterpulse ratios for EMI, Hamamatsu and Photonis PMT's.

One can see from these measurements that four out of six PMT's examined have afterpulse ratios of less than 5%. However, one EMI PMT and one Hamamatsu PMT have relatively large afterpulse ratios.

By looking at the arrival time distribution of these afterpulses, one can identify the ions that are causing them, since the delay of the afterpulse relative to the main pulse depends on the mass of the ion, for a give HV.

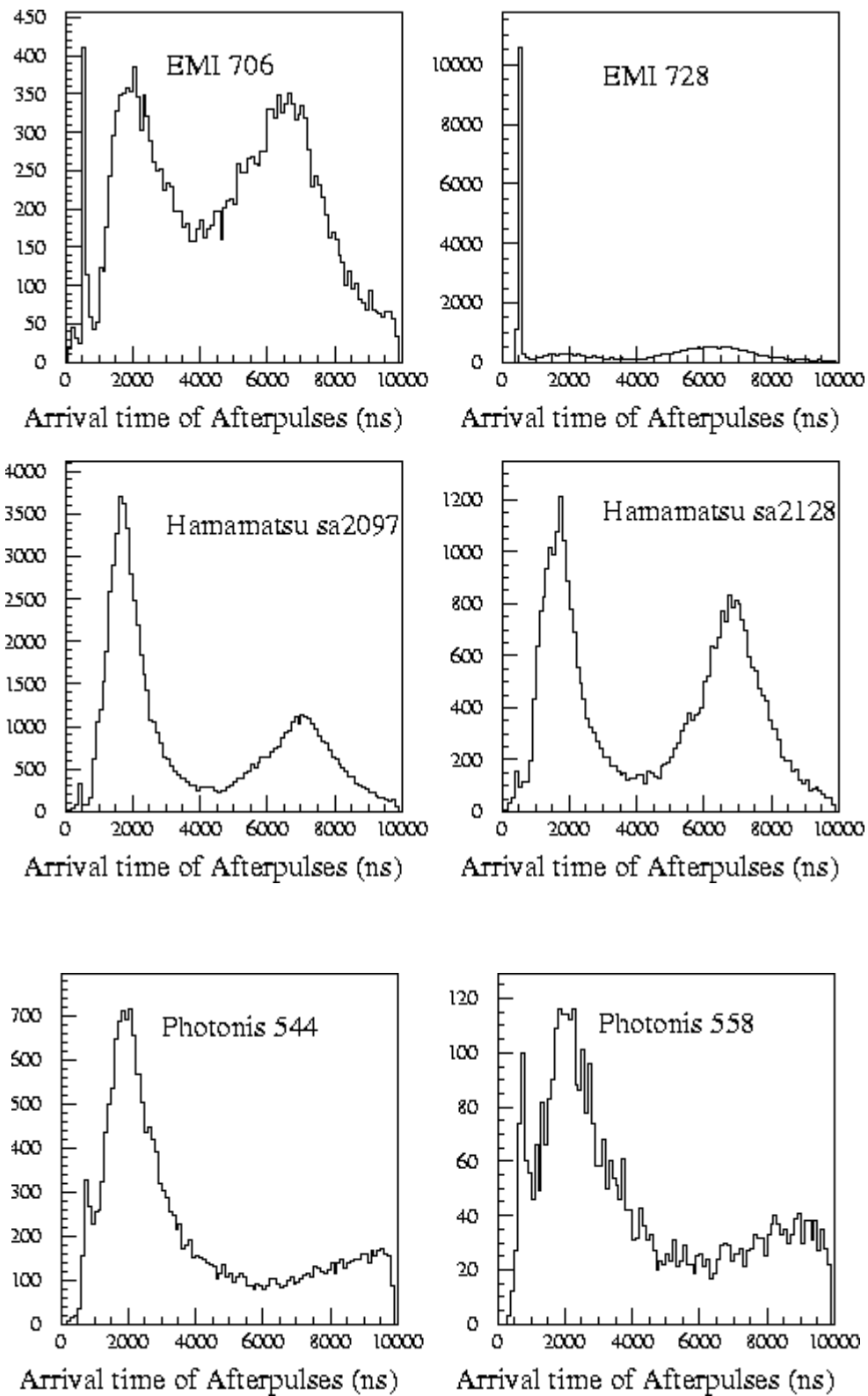


Figure 2.5.1 Distribution of Arrival times of afterpulses relative to the main pulse for different PMT's.

Figures 2.5.1 shows the distribution of the arrival times of the afterpulses for EMI and Hamamatsu PMT's. One could see the following features in all these distributions:

1. There is a peak around 7 μs in all the distributions, including EMI 706, which has a small afterpulse ratio. This peak could be from Cs^+ ions, which would be present in all PMT's with alkali photocathodes. Since these pulses arrive more than 5 μs after the main pulse, it is not a problem.
2. All PMT's show a peak around 2 μs . This peak could be from CH_4^+ ions. The relative height of this peak is the largest in Hamamatsu PMT's.
3. EMI 728, which has 7% afterpulse ratio, shows a large spike around 500 ns. This spike is also visible clearly on an oscilloscope. It could probably come from the light produced in the last dynodes.

3 Summary

The UCLA group has done a detailed testing of three different kinds of 8" PMT's: Hamamatsu R5912, EMI 9353KB, and Photonis XP1802/FLB (9") in order to evaluate their suitability for the Pierre-Auger Project. The results for all PMT's are summarized in Table 2 below.

Below are some conclusions one can draw from these measurements:

- All existing three types of PMT's are optimized for high gain (10^7) operation at high voltages around 1500 V. At a gain of around 10^5 , operating voltage becomes below 1000 V, and these PMT's are no longer linear.
- To be specific, Photonis has the best linearity, and Hamamatsu the worst. This is mainly because Hamamatsu has the lowest operating HV (700 V) for a gain of 10^5 .
- EMI has the highest quantum efficiency in the region of interest. One of the EMI PMT's has exceptionally high QE (19%) even at 300 nm. This could possibly be because of the difference in the glass bulb material.
- Hamamatsu is the most stable and quiet, as far as dark current and noise are concerned. This translates into long term reliability.
- Photonis PMT's become unstable at high voltages above 1500 V. This might be an indication of some undesirable discharges in dynodes.
- Photonis has the worst peak-to-valley ratio for the single photoelectron peak, because the first dynode is a foil type dynode. Hamamatsu exhibits the best peak-to-valley ratio.
- Of the six PMT's tested, one Hamamatsu (sa2097) and one EMI (728) PMT show a relatively large afterpulse ratio. The arrival time distribution of the afterpulses shows a spike around 500 ns for EMI 728 which could come from the light produced in dynodes being detected by the photocathode. Hamamatsu sa2097 shows a relatively large peak at 2 μs , which could come from CH_4^+ ions. This peak is present in all PMT's at a smaller level.
- All PMT's have dark pulse rates of less than 3 KHz.

	Spec	Hamamatsu R5912		Photonis XP1802/FLB		ETL 9353KB	
Diameter Photo-cathode Dynode	≥8"	8" Bialkali 10 Box +Linear		9" Bialkali 11 Foil+Linear		8" Bialkali 12 Linear	
Serial #		2097	2128	544	558	706	728
QE (%)							
at 300nm		3.9	3.2	5.4	10.8	3.3	19.0
at 350nm	>20	20.5	22.0	21.0	24.0	24.5	27.0
at 400nm	>20	20.2	22.8	19.6	22.2	23.9	24.5
HV (Volts)							
at Gain = 10 ⁵		750	650	820	800	750	900
at Gain = 10 ⁶		1000	850	1050	1000	950	1120
at Gain = 10 ⁷		1350	1150	1350	1350	1200	1500
Peak to Valley Ratio							
at Gain = 10 ⁷	>1.5	2.3	2.3	<u>1.2</u>	<u>1.4</u>	1.6	1.6
Dark Current (nA)							
at Gain = 10 ⁵		0.4	0.05	1.0	0.4	0.7	0.7
at Gain = 10 ⁶		1.3	0.4	2.4	1.3	1.5	3.0
at Gain = 10 ⁷	<10	7.0	3.4	<u>10.0</u>	9.0	9.2	<u>40.0</u>
Dark Pulse Rate after 1 Hr in Dark (KHz)	<10	2.6	1.7	2.3	2.4	0.9	2.9
After Pulse Ratio (%) (200-5000 ns)	<5	<u>5.8</u>	3.0	4.7	3.7	2.3	<u>7.1</u>
5% Non Linearity (mA)							
at Gain = 10 ⁵	>40		<u>10</u>	45			40
at Gain = 10 ⁶			45	60			60
at Gain = 10 ⁷			60	90			105

Table 2 - A summary of all 8" PMT measurements. **Bold face** numbers for a particular measurement indicate the *best* PMT(s) from the point of view of that particular quantity. The underlined numbers indicate the *worst* PMT(s) from the point of view of that quantity.

4 Conclusion

Linearity is an important criterion not satisfied by these PMT's for the Auger project, if we wish to operate them at low gain. This is not surprising, given the fact that these PMT's were designed to run at high voltage (high gain). To run them at a gain of 10⁵, we have to operate them at very low voltage, and there is not enough potential difference between the last dynodes to overcome

the space charge effect. Reduction in the number of dynode stages would probably be necessary if we wish to operate these PMT's at a gain of $\sim 10^5$ while maintaining good linearity up to 50 mA peak anode current. Another solution might be to tap a deep dynode to measure large signals with good linearity. However, the linearity of the dynode signal itself, and effect of the tap on the anode signal needs to be studied carefully. Such a study is in progress at UCLA.

In addition, one Hamamatsu and one EMI PMT show large afterpulse ratios that might not be acceptable. Since the shape of the pulses caused by through going muons and those caused from the EM showers are significantly different, the effect of afterpulse will not cancel exactly. A careful study of how the afterpulses will affect the energy measurement needs to be done.

5 Acknowledgements

We would like to thank Stephane Coutu and Jim Beatty at Penn State University for sending us six PMT's and sockets, and helpfully and promptly answering all our questions. We would also like to thank Dr. Vahe Ghazikhanian at UCLA for letting us use his circuit design for our LED pulsing circuit for the linearity system, and also for many useful discussion on how to improve it.

6 References

1. S. Coutu, J. Beatty, E. Fantozzi, J. Hartshorn; Auger Technical Note **GAP 99-045** (1999).
2. H. Bergeret, A. Cordier, P. Eschstruth, B. Merkel; Auger Technical Note **GAP 99-034** (1999).
3. B. Khrenov, Auger Technical Note **GAP 96-038** (1996).
4. P. V. Tkachenko, *I.I. Yashin*; Auger Technical Note **GAP 97-014** (1997).

- 2- The LED Driver generates fast analog pulses; sequentially output to two LED's contained in the Dark Box. One LED is pulsed, then the other, followed by a concurrent pulsing of both LED's. The LED Driver outputs a NIM trigger pulse with each LED driving pulse that is used for later triggering and gating.
- 3- PMT output in response to bursts from the LED's is passed through a Digital Oscilloscope, then an Attenuator, and finally fed into an ADC Module in the CAMAC Crate. From there the signal is digitized; results are put in a histogram and displayed via PC.

A.3 System Specifics

In this section, a detailed look at all system components will be given, including all devices, signal processing, and a piece-wise comprehensive sequential event flow catalog.

LED Driver & Periphery Electronics:

The LED-driving portion of the system is the critical component for achieving adequate linearity measurement precision. Demands of the measurement require that a subject PMT be hit in succession with two distinct, fast (short rise and fall time, short overall duration) bursts of light bearing staggered intensities of known proportion. PMT output is expected to follow light burst intensity in such a way that the ratio of the output peak current of the two successive PMT output signals will scale like the ratio of burst intensities when the PMT is operating within its linear region. If the ratio of the peak currents is not equal to the ratio of the burst intensities, the PMT is expected to be operating beyond its linear region. Thus, there is an immediate demand for a light source bearing these capabilities. In addition, because the PMT's undergoing tests at UCLA are intended for use as Cerenkov light detectors, optimum test sources should approximate light expected to be detected on site, namely near-UV, higher frequency blue light. To meet these specifications, blue LED's of varied intrinsic intensity per forward applied current were selected as the light source, while the driving circuit would be custom built based on an existing driver designed by Dr. Vahe Ghazikhanian and Yaozhong Shi, and in use in the UCLA Nuclear Physics Department.

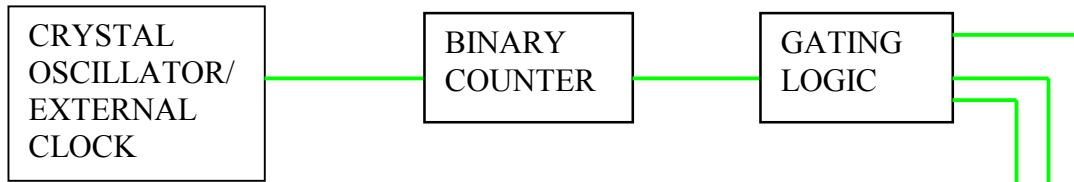
The need to generate two distinct bursts of light of staggered yet known intensities is fulfilled in an optimum way by the LED driving circuit. It drives two separate LED's on twin independent driving lines successively in time, then fires them both together for a total of three successive bursts of light incident on the PMT. Actual LED intensity is not known (though it can be estimated), nor required under this configuration, as an ADC readout of such a sequence allows the operator to see the PMT output after each LED is fired and when the two are fired together. The simple requirement that the sum of the outputs of the two LED's fired independently should equal that when they are fired together gives an appropriate condition for testing linearity. This configuration has the added advantage that decays in LED performance, variations in LED individual intensity, or poorly aligned LED firing do not affect the system's ability to measure linearity provided such events do not occur suddenly between successive pulses of any individual LED and the combined LED event of a single data cycle. All systematic error attributable to the light source is thus removed.

The circuit itself consists of twin driving lines pulsed by a common clocking and NIM sync generating line. Initially the circuit was clocked internally by a crystal oscillator, but was later modified to accept externally generated TTL clocking pulses as well. The output signal sequence is as follows:

- Upon appropriate load of a binary counter, triggering pulses are delivered to the NIM sync output driver and the first LED driving line. These initiate a pulse on the NIM sync line concurrent with a pulse on the first LED line (fires the first LED).
- Upon the next appropriate load of a binary counter, triggering pulses are sent to the NIM sync line and the second LED driving line with similar results (this time second LED fires).

- Upon the next appropriate load of a binary counter, triggering pulses are sent to the NIM sync line and both LED-driving lines (fires both LED's together).

CLOCKING NETWORK



DRIVING & SYNC LINES

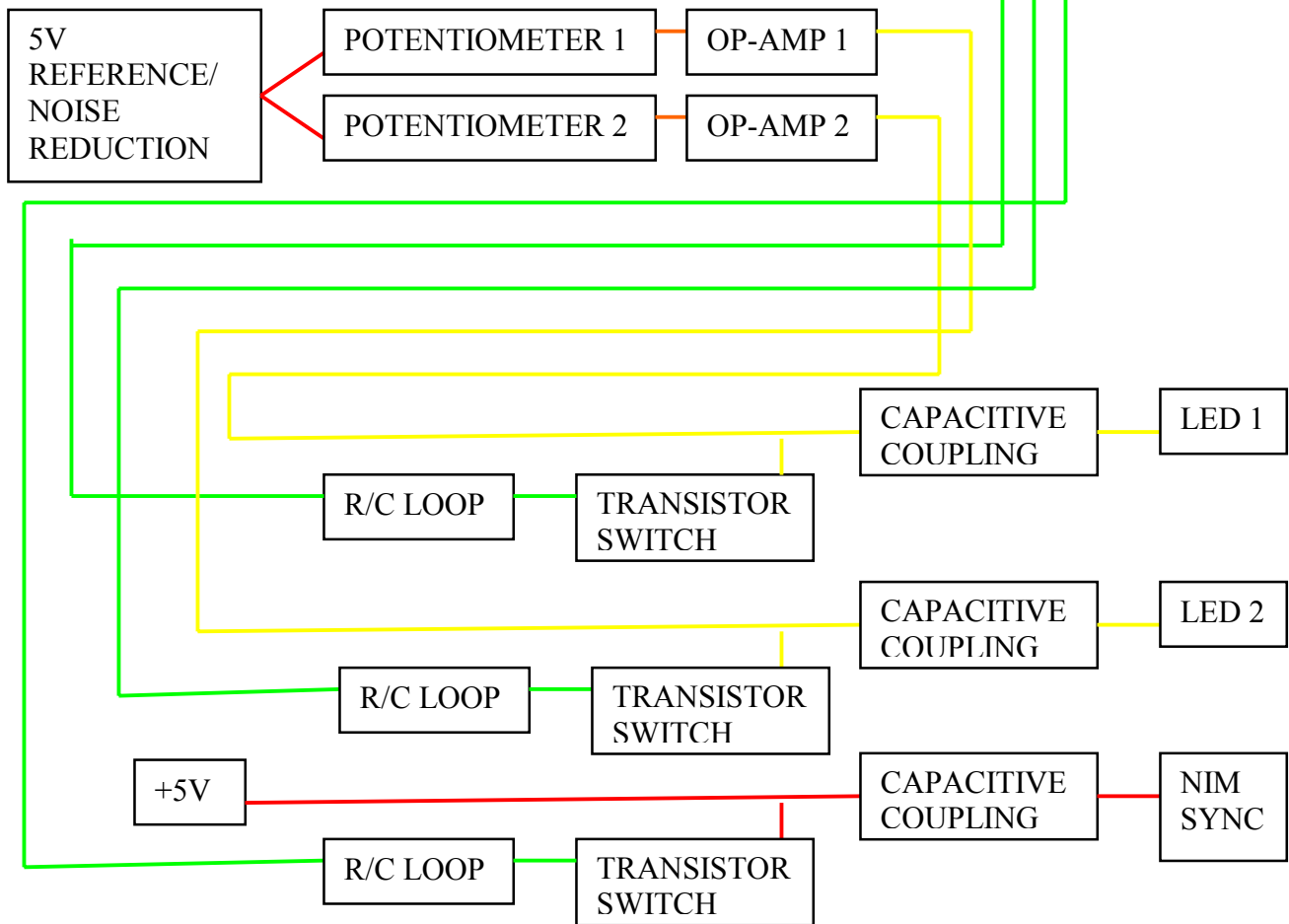


Figure A.3a – Skeleton Block Diagram/Flowchart of LED Driver circuit

TTL signal levels are standard, F-series gates are used for clocking signal processing, and driving line trigger signals are fed through an RC sub-circuit that precisely controls the time spread of the signal that activates the driver lines. The driver lines for the LED's are powered by twin op-amps whose voltage output levels (which will eventually drop over the LED's) are controllable via potentiometers on the non-inverting inputs. Positive op-amp voltage is converted to negative output driving pulses to the LED's by capacitively coupling the op-amp lines to the LED drive output lines. The op-amps are discharged with the incoming triggering signal (spread through the RC sub-circuit and generated by the clocking portion of the circuit) which closes a transistor switch (high speed NPN 2N2369), rapidly discharging the op-amp line for the duration of the triggering pulse, and generating a

fluctuation on the LED output lines causing them to fire. As mentioned, voltage levels of the output pulses are individually tunable via potentiometers, as is overall output level via potentiometer-controlled trim of the circuit's 5V reference chip. External monitoring of the DC levels on the op-amp lines is available via BNC even while the circuit is active. Thorough testing to assure low noise and proper grounding was conducted, as was meticulous efforts to ensure that there were no output level fluctuations on a given LED line when it fires alone versus when it fires in tandem. The LED Driver module employs standard BNC connections for all inputs and outputs, requires three input power voltages ($\sim +5.8\text{V}$, $+15\text{V}$, and -15V), and accepts external clocking or triggers internally (selectable by toggle switch). The module in use currently features dual independent complete driver units in a single case that allows a crosscheck of driver performance against its twin.

Currently the LED Driver is clocked externally to allow for rapid changes in overall data acquisition cycle rate if necessary, though the rate has settled at approximately 250 Hz and has remained there for all linearity testing. Future upgrade/second generation LED Driver devices will likely return to the use of internal clocking via crystal oscillator that will maximize time-stability of the entire circuit and ultimately govern and fix the data cycle rate. The frequency of the oscillator has yet to be finalized, and is somewhat dependent on the maximum data cycle rate achievable by the DAQ software which will also undergo upgrade.

Several LED's are available for use in the system, all of which are blue-band, but vary in their other properties:

- Type 1 – Sun LED L934MBDL – 3.0mm-T1 - Blue Diffused (SiC) - 430nm - 50mcd/I_F - 60° Viewing Angle
- Type 2 – Sun LED LUB53D – 5.0mm-T1^{3/4} - Blue Diffused (SiC) - 430nm -30mcd/I_F - 60° Viewing Angle
- Type 3 – Sun LED LMB90W – 5.0mm - Super Blue Clear (SiC) - 450nm - 500mcd/I_F - 20° Viewing Angle
- Type 4 – Panasonic LNG992CFBW – 5.0mm-T1^{3/4} - High Brightness Blue Clear - 470nm - 1500mcd/I_F - 15° Viewing Angle

Currently the system is running with two Type 3 LED's in place connected to the LED Driver via standard BNC cables through bulkhead connectors in the wall of the Dark Box. Each LED is wired with a 50 Ω current limiting and terminating resistor on the grounded side of the diode, which has been wired to accept negative bias pulses. The voltages on the LED's individually are staggered such that each of the two outputs a different intensity. Some data was taken previously using the Type 4 LED's in identical configuration, as were some test runs using a combination of Type 3 and 4 LED's.

The LED Driver, as mentioned, is presently clocked externally. A Phillips Scientific Model 794 Quad Gate/Delay Generator single-width NIM module is employed as the clock. Two of its four stages are cross-triggered via the TRIGGER input and DELAY output, and the WIDTH knob of each stage is set such that one stage's duration generates the "high" portion of a square wave via its TTL output, while the second stage functions as "downtime" on the first stage's TTL output for the duration of the second stage. The overall product is a symmetric square wave pulse train formatted in TTL, which is fed via BNC or LEMO into the EXTERNAL CLOCK input on the LED Driver. Currently, the WIDTH knobs on the Gate/Delay Generator are tuned so as to generate a pulse train of frequency necessary to result in an end-product data cycle rate of around 250Hz. The NIM bin currently used to house and power the module is an Ortec 401A.

Two laboratory bench power supplies power the LED Driver. The +5.8V V_{CC} power is provided by one half of a Lambda Model LQD-421 Dual Regulated Power Supply with front panel dial-in voltage control set to +5.8V, face-wired common ground establishment on the negative output, and power delivered to the LED Driver via banana-to-BNC adapter and BNC cable. A Tektronix PS280 DC Power Supply provides the +15.0V and the -15.0V to the LED Driver via similar hook-ups.

During the course of testing the Driver, the PS280 has shown to be very stable when the op-amps in the Driver circuit are activated to drive the LED lines both independently and simultaneously. Though the burst width of the LED driving pulses is short (about 30ns), if the power supply was unable to keep the lines biased, it would go into “constant current mode” as a safety against the effective short it would see while the op-amps are active. This behavior was not observed, and the output pulses of the LED Driver are extremely uniform and symmetrically shaped, as well as remarkably stable.

Dark Box & PMT Housing:

Subject PMT's are housed and mounted individually inside a 3 cubic-foot wooden Dark Box (painted flat black) which is constantly monitored for light leaks. Inside the box the tubes are placed on foam pads horizontally (in a plane parallel to the earth's surface) and faced at the light source. All cabling is done via BNC bulkhead connectors in the wall of the box. A given tube is fitted with a base custom-constructed at UCLA and (presently) built to company-recommended specs for pulsed linearity testing. This includes a tapered resistor chain designed to boost the final few stages in proportion to middle-stage dynode drop potentials. Tubes are tested with both positive and negative high voltage bases. The next upgrade will include the addition of a variable potential base. This device, which is complete but awaits proper interface to the Dark Box, will allow for full-range dynode potential control on the last three dynodes of all subject PMT's, as well as variable potential control of the drop between the cathode and first dynode of all subject PMT's. It will accept positive or negative high voltage so that a full range of tests can be performed. It is expected that this device will allow for the optimization of the dynode chain resistor values, and/or the possible elimination of dynode stages deemed excessive for the linearity and operating gain parameters specified for the Auger Detector.

The light source, consisting of the two LED's currently in use mounted in a collimating/mixing aluminum guide block and fixed to an adjustable lift anchored to an aluminum plate on the floor of the Dark Box, is aimed directly at the subject PMT at a range of approximately 1 foot. The source block is butted up flush with a circular neutral density filter wheel that serves as the primary intensity attenuator through a range of any given PMT's testing cycle. (The two LED's are set to staggered initial intensities by the Driver's voltage control, and then unaltered for the duration of any given PMT's test run. Further attenuation variability is delivered compliments of the filter wheel.) The filter has been aligned such that typically the PMT is saturated when it is at zero attenuation, and no light reaches the PMT when it is at maximum attenuation. Recently the filter wheel was fitted to an externally computer-controlled stepping motor that allows for easy attenuation tuning without opening the Dark Box. Presently there is some progress to be made in precise calibration of the motor movements. Such efforts are underway, and the next iteration of the system is expected to have fine-precision control of motor movement, and total computer-controlled spatial orientation angle of the filter wheel. Improvements are scheduled in the light source collimating block and the mixing/diffusing of the LED's as well, with plans of uniformly illuminating the entire forward surface of the test PMT's rather than shining a small-angle beam into various positions on the surface of the PMT's.

High Voltage Power Supply:

The linearity system currently uses a Stanford Research Systems Model PS350 for providing high voltage to subject tubes. It is polarity-variable and has shown to be more stable and precise than initially evaluated NIM Ortec analog meter supplies. High voltage is fed to the Dark Box via SHV bulkhead connectors and high voltage coaxial cables. Similar devices are computer-controlled in other PMT test stations, and eventually the linearity system will likely go to computer-controlled high voltage via GPIB to the PS350.

Data Acquisition:

The signal-out line from the subject PMT is standard BNC and is passed through the wall of the Dark Box via BNC bulkhead connector. The anodes (signal-out) of the bases used in recent testing with negative high voltage have all been floating relative to the local base divider ground (ultimately grounded through the ADC or scope), and in the case of positive high voltage bases, the floating signal-out line is capacitively coupled to the anode which sits at +HV. The signal line is passed over one channel of a Tektronix TDS 654C 5GS/s 500MHz Digitizing Oscilloscope with input impedance set to $1M\Omega$ so as to minimally affect its amplitude while reading the PMT's output peak voltage (to be converted to output peak current) and signal shape in time. Using a BNC T-junction connector, the signal is passed from the scope to a Lecroy Research Systems Model A101 Attenuator which has 50Ω terminations on its both its input and output lines, and can attenuate input signals by as much as a factor of ten variably controllable via a knob on the device's housing. Depending on the initial strength of the signal, a second fixed 10x Tektronix 011-0059-01 50Ω -terminated attenuator is sometimes added to the signal line after leaving the Lecroy Attenuator. Following attenuation, the signal is fed into one channel of (at present) a Lecroy 2249W ADC mounted in a Kinetic Systems Model 1502 CAMAC Crate. The system is controlled via a Wiener CC16 Crate Controller ribbon-cabled to a Wiener PC16 ISA interface card mounted inside a desktop PC running Windows 98 operating system software. A Wiener-provided driver embedded within a National Instruments LabVIEW VI data acquisition program custom written for the linearity system is employed as the DAQ readout and control

The LED Driver unit initiates triggering. NIM marker pulses are output on the NIM SYNC line from the Driver in coincidence with each output pulse appearing on an LED driving line. (The Driver has been adjusted to output the NIM marker very close in time to the output driving pulses, thus external delays to align signal and gate have been minimized to avoid the use of long cables which have been shown to degrade signal quality.) This signal is fed into a Lecroy Model 623B Octal Discriminator single-width NIM module mounted in the aforementioned Ortec 401A NIM bin, and processed above threshold to generate a true NIM gate pulse. Two outputs of the Discriminator are engaged; one feeds the NIM gate as a trigger signal to the TRIGGER input of a free stage of the aforementioned Phillips Scientific Model 794 Quad Gate/Delay Generator, while the second output of the Discriminator feeds the "A" input of a Lecroy Model 365AL 4-Fold Logic Unit single-width NIM module also housed in the Ortec 401A bin. The gate fed to the Gate/Delay Generator is delayed, output on that module's DELAY output line, and fed into the 4-Fold Logic Unit's "B" input. The Logic Unit is programmed with a Boolean "OR" coincidence between its "A" and "B" inputs, and one of its output lines is used to drive the fourth and final stage of the Phillips Scientific Gate/Delay Generator. This additional Logic Unit stage is required as a temporary satisfaction of the desire to monitor pedestal during a data run simultaneously with the usual three LED burst events of a standard data cycle. The LED Driver outputs NIM triggers only when it activates an LED driving line as well; thus, under normal operating conditions, pedestal is only measurable when the Driver is not actively running (i.e., during a data run). Ideally, pedestal should be monitored throughout the run, intermittent with actual LED burst events. By feeding the additional output of the Discriminator to the Gate/Delay Generator, and using the delay feature on that module, an additional NIM trigger pulse intermittent in time following the usual three LED burst event triggers of a given data cycle is created. The additional NIM pulse is integrated with the original train being fed into the Logic Unit directly from the Discriminator, and the "OR" coincidence established between the two inputs results in single NIM gate pulse train output on the Logic Unit's output line. [This train now includes three successive gate pulses corresponding to the three burst events (the first LED firing, the second, and then the combined event) followed by a fourth gate pulse which corresponds to PMT downtime (no LED event) and allows for an integrated measurement of the pedestal with burst data. (Data in a histogram now typically shows three event peaks and pedestal all on a single plot.)] Gate pulses are equidistant in

time, and as mentioned, are fed lastly back into the final available stage of the Gate/Delay Generator where the output GATE line is sent to the ADC's input GATE channel. This final pass through on the Gate/Delay Generator allows for the selectable duration of the actual gate used for data reads by way of the WIDTH knob on the panel face. Currently, before sending the final gate signal line to the ADC, it is passed through a 1M Ω -terminated input to verify gate stability (which has been an issue) and time alignment with the PMT output signal. The next iteration of the Driver circuit will likely be modified to include the generation of an off-event gate so as to reduce the external network of gate signal routing presently employed to achieve the same ends. In addition, there has been a growing desire to register data cycle events individually as part of a four-event block so as to identify all iterations of, say LED one firing alone, etc. By "tagging" individual events and distinguishing them from surrounding events, occasions where peaks on resultant histograms overlap can still be resolved by looking at each peak one at a time through separate channels in the ADC. This feature will likely be hardwired in to the next generation LED Driver circuit.

System Concerns & Performance Verification:

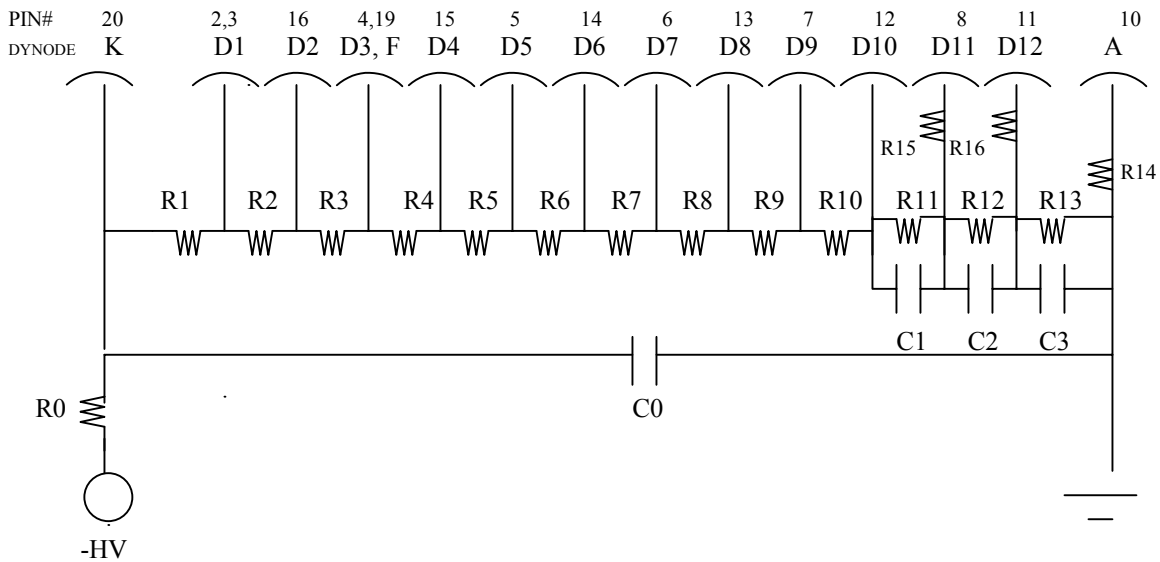
The LED Driver underwent extensive scrutinization to ensure that it did not import any inherent or systematic non-linearity into the measurement. LED driving voltages on each line absolutely must remain identical during both individual events the combined event. Monitoring of the actual driving voltages initially showed dips in voltage on both lines during the combined event relative to the individual events. This was determined to be a result of fluctuations in the local ground line in the circuit near the driving line transistor switches, and not a function of power supply's inability to maintain the line voltage during a combined event. Currently, the LED Driver has proven to be extremely linear, as verified not only in scope traces of driving pulse voltages and shapes, but also in the reproduction of known linearity curves of such inordinately linear phototubes as Hamamatsu's R2490 Fine Mesh PMT which remains comfortably linear up to nearly 1 ampere of peak current.

Appendix B

B.1 Base Design for EMI PMT's (Negative HV)

EMI 9353 KB

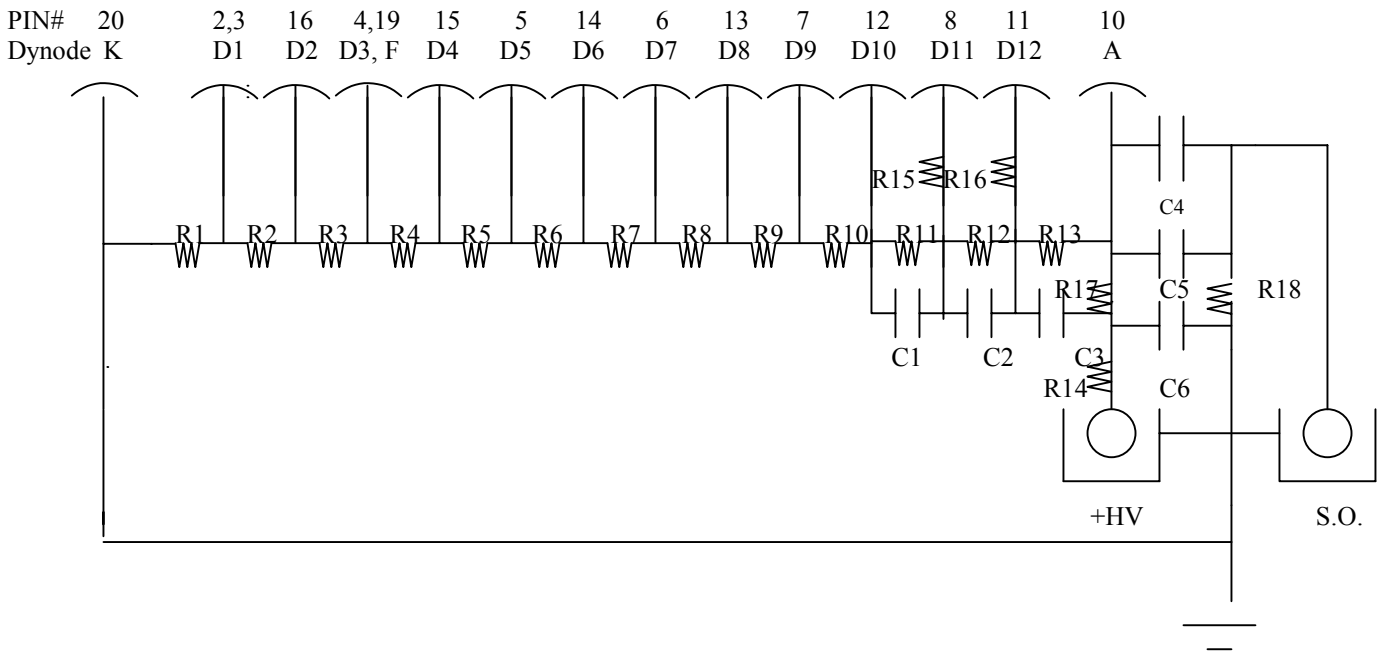
Dynodes:	K	d1	d2	d3	d4 ... d8	d9	d10	d11	d12	a
Resistor proportions	9.1R	1.5R	1.5R	R	...	R	2R	3R	4R	3R
Voltage Drops (V)	450	73.8	73.8	49.2	...	49.2	98.4	147.6	196.8	147.6



- R0 = 10 kΩ
- R1 = 1.097 MΩ
- R2, R3 = 180 kΩ
- R4... R9 = 120 kΩ
- R10 = 240 KΩ
- R11, R13 = 360kΩ
- R12 = 480 kΩ
- R14 = 100kΩ
- R15, R16 = 50Ω

- C0 = 4700 pF
- C1, C2, C3 = .01 μF

B.2 Base Design for EMI PMT's (Positive HV)



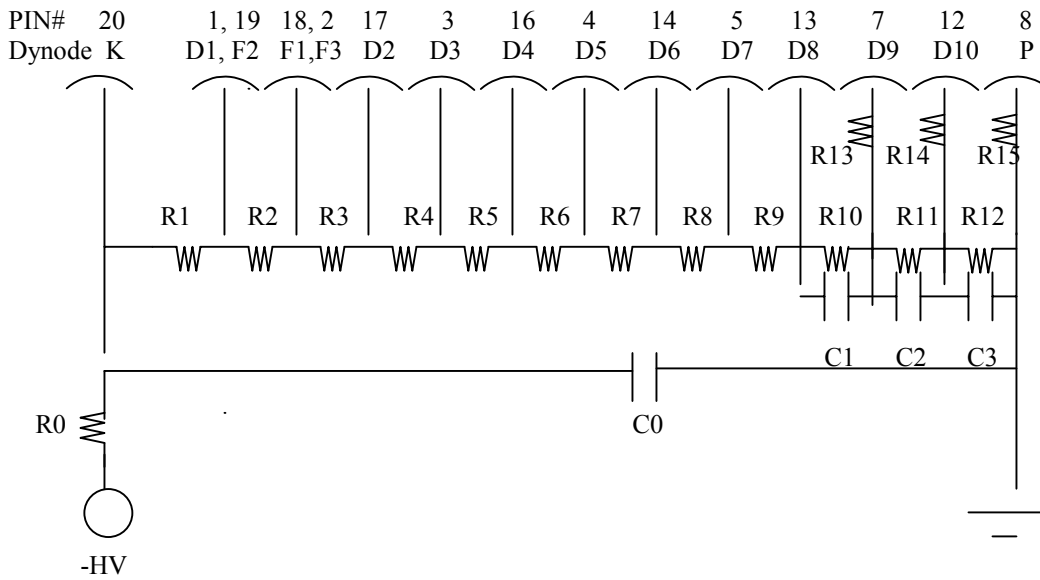
$R0 = 10 \text{ k}\Omega$
 $R1 = 1.097 \text{ M}\Omega$
 $R2, R3 = 180 \text{ k}\Omega$
 $R4 \dots R9 = 120 \text{ k}\Omega$
 $R10 = 240 \text{ k}\Omega$
 $R11, R13 = 360 \text{ k}\Omega$
 $R12 = 480 \text{ k}\Omega$
 $R15, R16 = 50 \text{ }\Omega$
 $R17, R18 = 100 \text{ k}\Omega$
 $R14 = 10 \text{ k}\Omega$

$C4, C5, C6 = 4700 \text{ pF}$
 $C1, C2, C3 = .01 \text{ }\mu\text{F}$

B.3 Base Design for Hamamatsu PMT's (Negative HV)

R5912

Dynodes	K	D1, F2	F1, F3	D2	D3	D4	D5	D6	D7	D8	D9	D10	P
Resistor proportions		11.3R	.6R	3.4R	5R	3.33R	1.67R	R	1.2R	1.5R	2.2R	3R	2.4R
Voltage Drops (V)		542	28.8	163	240	160	80	48	57.6	72	105.6	144	115.2



- R0 = 10 kΩ
- R1 = 1.356 MΩ
- R2 = 72 kΩ
- R3 = 408 kΩ
- R4 = 600 kΩ
- R5 = 400 kΩ
- R6 = 200 kΩ
- R7 = 120 kΩ
- R8 = 144 kΩ

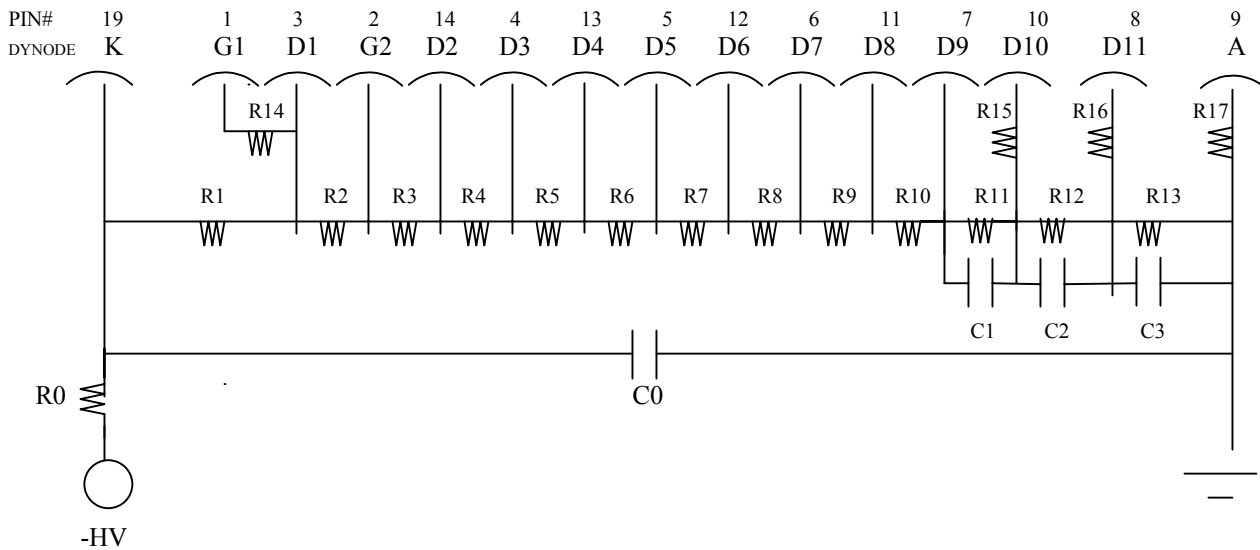
- R9 = 180 kΩ
- R10 = 264 kΩ
- R11 = 360 kΩ
- R12 = 288 kΩ
- R13, R14 = 50 Ω
- R15 = 100 kΩ

- C1, C2, C3 = .01 μF
- C0 = 4700 pF

B.5 Base Design for Photonis PMT's (Negative HV)

XP1802

Dynodes:	K	G1	D1	G2	D2	...	D5	D6	D7	D8	D9	D10	D11	A	
Resistor proportions		.2R		R	3R	R	...	R	1.25R	1.25R	1.5R	2.25R	2.5R	3R	2.75R
Voltage drops (v)		9.6		48	144	48	...	48	60	60	72	108	120	144	132
		480													



$R0 = 10 \text{ k}\Omega$
 $R1 = 1.2 \text{ M}\Omega$
 $R2 = 120 \text{ k}\Omega$
 $R3, R12 = 360 \text{ k}\Omega$
 $R4... R6 = 120 \text{ k}\Omega$
 $R7, R8 = 150 \text{ k}\Omega$
 $R10 = 270 \text{ k}\Omega$

$R11 = 300 \text{ k}\Omega$
 $R13 = 330 \text{ k}\Omega$
 $R14 = 24 \text{ k}\Omega$
 $R15, R16 = 50 \text{ }\Omega$
 $R17 = 100 \text{ k}\Omega$
 $R9 = 180 \text{ k}\Omega$
 $C0 = 4700 \text{ pF}$
 $C1, C2, C3 = .01 \text{ }\mu\text{F}$

